

1-1-1988

**Late Holocene earthflows of the Willard Playa/dune complex,  
Estancia Valley, New Mexico; a geomorphic response to climatic  
change**

Kurt A Goebel  
*University of Nevada, Las Vegas*

Follow this and additional works at: <https://digitalscholarship.unlv.edu/rtds>

---

**Repository Citation**

Goebel, Kurt A, "Late Holocene earthflows of the Willard Playa/dune complex, Estancia Valley, New Mexico; a geomorphic response to climatic change" (1988). *UNLV Retrospective Theses & Dissertations*. 52.

<http://dx.doi.org/10.25669/cb53-21sh>

This Thesis is protected by copyright and/or related rights. It has been brought to you by Digital Scholarship@UNLV with permission from the rights-holder(s). You are free to use this Thesis in any way that is permitted by the copyright and related rights legislation that applies to your use. For other uses you need to obtain permission from the rights-holder(s) directly, unless additional rights are indicated by a Creative Commons license in the record and/or on the work itself.

This Thesis has been accepted for inclusion in UNLV Retrospective Theses & Dissertations by an authorized administrator of Digital Scholarship@UNLV. For more information, please contact [digitalscholarship@unlv.edu](mailto:digitalscholarship@unlv.edu).

## INFORMATION TO USERS

The most advanced technology has been used to photograph and reproduce this manuscript from the microfilm master. UMI films the text directly from the original or copy submitted. Thus, some thesis and dissertation copies are in typewriter face, while others may be from any type of computer printer.

The quality of this reproduction is dependent upon the quality of the copy submitted. Broken or indistinct print, colored or poor quality illustrations and photographs, print bleedthrough, substandard margins, and improper alignment can adversely affect reproduction.

In the unlikely event that the author did not send UMI a complete manuscript and there are missing pages, these will be noted. Also, if unauthorized copyright material had to be removed, a note will indicate the deletion.

Oversize materials (e.g., maps, drawings, charts) are reproduced by sectioning the original, beginning at the upper left-hand corner and continuing from left to right in equal sections with small overlaps. Each original is also photographed in one exposure and is included in reduced form at the back of the book. These are also available as one exposure on a standard 35mm slide or as a 17" x 23" black and white photographic print for an additional charge.

Photographs included in the original manuscript have been reproduced xerographically in this copy. Higher quality 6" x 9" black and white photographic prints are available for any photographs or illustrations appearing in this copy for an additional charge. Contact UMI directly to order.

# U·M·I

University Microfilms International  
A Bell & Howell Information Company  
300 North Zeeb Road, Ann Arbor, MI 48106-1346 USA  
313/761-4700 800/521-0600



Order Number 1338260

**Late Holocene earthflows of the Willard Playa/dune complex,  
Estancia Valley, New Mexico; a geomorphic response to climatic  
change**

Goebel, Kurt A., M.S.

University of Nevada, Las Vegas, 1989

**U·M·I**  
300 N. Zeeb Rd.  
Ann Arbor, MI 48106



**LATE-HOLOCENE EARTHFLOWS OF THE WILLARD PLAYA/DUNE  
COMPLEX, ESTANCIA VALLEY, NEW MEXICO; A GEOMORPHIC  
RESPONSE TO CLIMATIC CHANGE**

By

Kurt A. Goebel

A thesis submitted in partial fulfillment  
of the requirements for a degree of

Master of Science

in

Geology

Department of Geoscience  
University of Nevada, Las Vegas  
August, 1989

The thesis of Kurt A. Goebel for the degree of  
Master of Science in Geology is approved.



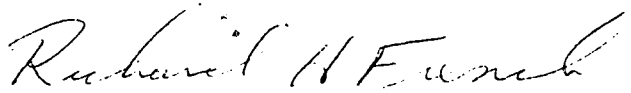
---

Chairperson, Frederick W. Bachhuber, Ph.D.



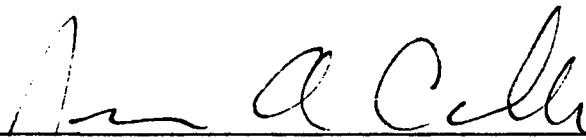
---

Examining Committee Member, David L. Weide, Ph.D.



---

Examining Committee Member, Richard French, Ph.D.



---

Graduate Faculty Representative, James Cardie, Ph.D.



---

Graduate College Dean, Ronald W. Smith, Ph.D.

University of Nevada, Las Vegas  
August, 1989

LATE-HOLOCENE EARTHFLOWS OF THE WILLARD PLAYA/DUNE  
COMPLEX, ESTANCIA VALLEY, NEW MEXICO; A GEOMORPHIC  
RESPONSE TO CLIMATIC CHANGE

By

Kurt A. Goebel

**ABSTRACT**

Late-middle to late Holocene dune sediment that overlies Pleistocene lacustrine sediment marks the onset of xeric conditions in the Estancia Valley, central New Mexico. Two distinct eolian episodes are recognized, one of which culminated in the development of the modern deflation basin and dune complex. Incised into the underlying lacustrine sediments, the deflation basins are enclosed by parabolic dunes that are composed of clay pellets and gypsum derived from the underlying sediment.

Located on the in-facing duneslopes of the deflation basins, the most striking geomorphic feature of this dune complex are numerous elongated scars. These relict scars, exhibiting erosionally-modified headscarps and lateral margins, document a geomorphically distinct earthflow event. Arroyos that cut into flow scars expose eolian earthflow sediment overlying lacustrine deposits. In the zone of depletion, erosional-flow evidence reveals flamed-load structures, channels, and rip-up clasts of lacustrine sediments. This suggests that the lacustrine sediments acted as the main slip surface for the water-saturated, clay-rich dune sediments. In the zone of accumulation, depositional flow evidence, which has mostly been removed by deflation and lateral expansion of the modern playas, reveals laminations and lithic-rich horizons derived from the

underlying lacustrine section.

The large number of geomorphically similar earthflow scars of probable similar age, are believed to represent a more mesic climatic fluctuation within the late Holocene of the Estancia Valley.

## TABLE OF CONTENTS

Introduction.....	1
Purpose and Significance.....	1
Geographic Setting.....	2
Topography.....	2
Vegetation and Soils.....	4
Climate.....	6
Geologic Setting.....	7
Late Tertiary and Quaternary History.....	8
Early to Middle Holocene History.....	11
Middle to Late Holocene History.....	13
Slope Movement Processes and Earthflows.....	13
Slope Movements.....	15
Classification.....	17
Morphology.....	19
Style of Motion.....	19
Increased Effective Moisture.....	20
Pore Pressures and Loading.....	20
Hydraulic Conductivity.....	24
Liquidization.....	21
Mechanical Properties.....	21
Mohr-Coulomb Criterion.....	22
Effective Stress.....	23

Earthflows of The Willard Playa/Dune Complex.....	24
Lithology of the Earthflow Sediment.....	24
Origin of Sediments.....	27
Geomorphic Evidence.....	28
Morphology.....	28
Morphometry.....	30
Stages of Preservation.....	32
Sedimentary Evidence.....	35
Erosional-Flow Evidence.....	35
Depositional-Flow Evidence.....	39
Particle-Size Analysis.....	43
Methodology.....	43
E-28 Bucket-Auger Samples.....	45
Outcrop-flow Samples Samples.....	45
Sieve Analysis Summary.....	48
Geohydraulic Conditions Affecting Stability.....	48
Groundwater.....	49
Loading.....	49
Pore Pressure.....	49
Hydraulic Conductivity.....	50
Clay and Water Interaction.....	50
Implications.....	51
Alternative Interpretations.....	52

Holocene History and Development of the Willard Playa/Dune Complex.....	53
Deflation Basin and Dune Development Phase.....	53
Deflation Basin-Fill Phase.....	54
Earthflow Phase.....	57
Modern Phase.....	60
Deflation of Earthflow Sediment.....	60
Arroyo Cutting.....	61
Aggradation.....	62
Lateral Expansion and Deflation.....	64
Conclusions.....	65
Regional Implications.....	67
Late-Middle Holocene.....	68
Late Holocene.....	70
Summary.....	73
References Cited.....	74
Appendices.....	80

## ILLUSTRATIONS

Figure 1. Location map of the central Estancia Valley.....	3
2. Plan view and cross-section of playa E-28, 29 and 30 .....	5
3. Quaternary stratigraphy in the Estancia Valley.....	10
4. Holocene time table and the proposed late-middle to late-Holocene stratigraphy.....	12
5. Photograph of dated soil horizon and contact between Meinzer and Willard dunes.....	14
6. Slope movement classification.....	16
7. Plan view of type 1, 2 and 3 scars at E-28.....	25
8. Photomicrograph of typical earthflow sediment.....	26
9. Photograph showing flow scar morphology.....	29
10. Photograph of reactivation scarp.....	31
11. Photograph of a type 1 flow scar.....	34
12. Diagrammatic cross section of depositional and erosional flow regimes.....	36
13. Photographs revealing erosional-flow evidence.....	38
14. Photograph of exposed axial channel.....	40
15. Photograph of oblique view showing flow scar, ridge, and outlier.....	41
16. Photographs revealing depositional-flow evidence.....	42
17. Comparison of wet versus dry sieve analysis for typical dune material.....	44
18. Cross section and bucket-auger data for E-28-F2.....	46
19. Block diagram of dune development and basin-fill phase.....	55
20. Photograph showing basin-fill evidence.....	56
21. Block diagram of earthflow and modern phase.....	58

22. Photograph of unstable arroyo walls.....	63
23. Photograph of wind-carved exposure along northeast margin of E-32.....	66
24. Chart of geographic and climatic correlations.....	69
Table 1. Morphometry of several flow scars.....	33
Appendix 1. Dune sediment geochemistry.....	80
2. Sieve data.....	81
Plate 1. Surficial geologic map.....	82

## ACKNOWLEDGMENTS

I dedicate this paper to all of my colleagues, with whom I have shared so many memorable experiences. I especially thank my advisor, Frederick W. Bachhuber, who provided consultation, guidance and encouragement. His sincere interest in the field as well as on editing the manuscript are greatly appreciated. I am also grateful to David L. Weide for his guidance and constructive technical editing. I thank committee members Richard French from the Desert Research Institute and James Cardle from the Department of Civil and Mechanical Engineering for their suggestions.

I sincerely appreciate funding by the UNLV Graduate Student Association, and the scholarship and teaching assistantship provided by the Geoscience Department. Thanks to my friend Terry for his constant support and encouragement and Dann Halverson for his field assistance. Finally, a very special thanks to my wife-to-be, Trish, whose newly found presence in my life provided invaluable inspiration.

## INTRODUCTION

Late Holocene climate in the Estancia Valley, central New Mexico, produced a sequence of playa-floored deflation basins and associated parabolic dunes consisting of clay pellets and gypsum crystals. The dune slopes facing the deflation basins are often scarred by arcuate depressions. These depressions are believed to be relict earthflow scars that formed during a time when increased precipitation produced slope instability and mass wasting. The objective of this study is to demonstrate that these arcuate depressions are the result of earthflow events and that they were produced during climatic conditions different from those of the present.

## PURPOSE AND SIGNIFICANCE

Previously thought to be deflation features, F.W. Bachhuber (personal communication, 1986) suggested that the arcuate depressions are the result of a mass-movement phenomena that hold paleoclimatic significance. Earthflows, which are attributed to highly-fluidized, mass-movement of fine-grained weathered rock and soil are believed to be responsible for the arcuate depressions. This study, the first to describe the earthflow features, suggests that water, derived from a climatic episode more mesic than the present or the time of dune formation, induced these flows by saturating and destabilizing the clay portion of the dunes. The basic hydraulic and physical factors that produced the earthflows are also described. I believe that the earthflow event in the Estancia Valley documents a late Holocene short-term climatic oscillation that may have regional significance in the southwest.

## **GEOGRAPHIC SETTING**

The Estancia Valley is located in Torrance County, central New Mexico, approximately 95 km southeast of Albuquerque (Fig. 1). The elongated valley extends 100 km north-south and is 50 km wide at its maximum east-west dimension. The total area of the valley is approximately 6,000 km<sup>2</sup>. The study area that contains the deflation basin/dune complex is located in the south-central portion of the valley. This area comprises approximately 180 km<sup>2</sup> or 4% of the valley proper. Access to the study area is via State Highway 41. The highway parallels the study area on the east between the towns of Estancia and Willard. From Willard, Highway 60 trends eastward directly through the southernmost portion of the field area. An abandoned section of Highway 60 and numerous ranch roads provide further access to the interior of the deflation basin/dune complex.

### **Topography**

The present landscape of the study area is dominated by playa-floored deflation basins and adjacent parabolic dunes that Bachhuber (1971) termed the Willard Playa Complex. There are over 80 playa-floored deflation basins (numbered sequentially by Bachhuber, 1971) ranging in shape from semi-circular to elongate and in size from approximately 1 to 20 km long. The largest of these, Laguna del Perro, forms a distinct north-south basin that extends the length of the complex. Most of the deflation basins occur on the east side of Laguna del Perro and are confined by the lowest distinct strandline that is probably of Lake Willard origin. At the outer margin of the complex, deflation basins are incised only several meters below the general valley floor (1,860 m), whereas at the center of the complex, basins are incised to a depth of over 10 m into the underlying lacustrine sediments. The parabolic dunes adjacent to each of the

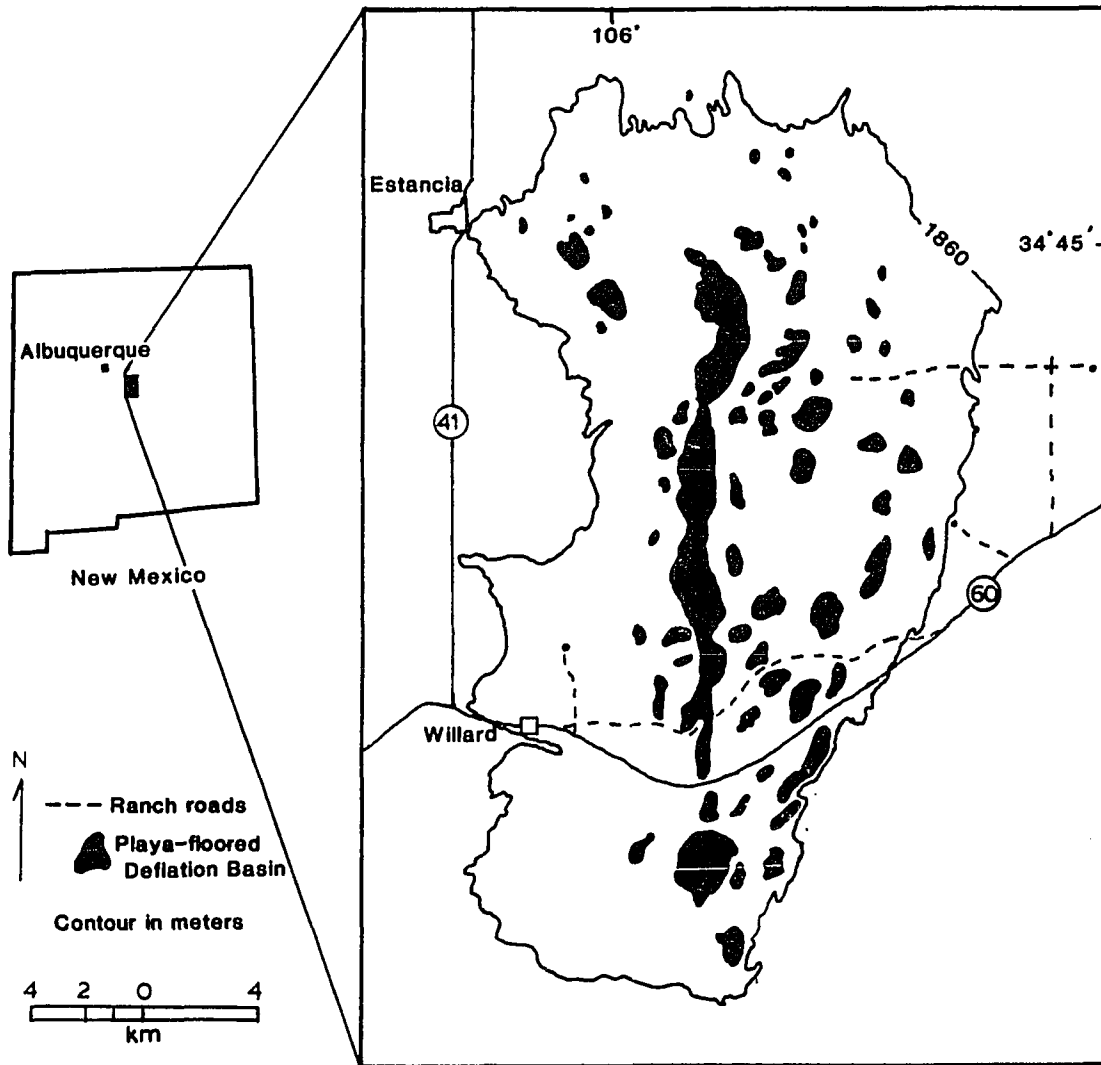


Figure 1. Index map for the Willard Playa/Dune Complex located within the central Estancia Valley, New Mexico.

deflation basins are best developed on the northeast margin of each basin. The dunes attain a height of up to 30 m at the central portion of the complex producing a maximal relief of 40 m from dune crest to playa floor (Fig. 2).

Playa-floored deflation basins and clay-rich dunes are documented in the west and southwest (Osterkamp and Wood, 1987; Weide, 1975; Price, 1963; Roth, 1960), and gypsum dunes occur at White Sands National Monument, New Mexico. However, the only location that exhibits the dual clay and gypsum composition, as well as deeply incised deflation basins, associated with large, high-relief parabolic dunes is in Australia. Bowler and Wasson (1986), Bowler and Teller, (1986), Bowler (1976; 1986), and Wasson (1983), document deflation basins and dune complexes analogous to those described here in the Estancia Valley.

### **Vegetation and Soils**

Vegetation of the Estancia Valley is diverse and varies according to climate and soil. The climatic zones are topographically controlled and are subdivided into the hot, dry, valley floor, that contains the dune complex, the valley alluvial slopes, and the upper montane slopes. In addition to climate, soil texture and composition act as controls on vegetation.

The flat interdune area contains a clay-rich soil that, according to the United States Soil Conservation Service soil classification scheme (Seventh approximation, 1960), is an aridic ustorthid. In general, this area is mapped as the Willard loam (Boulier and others, 1970). Based on identification by Bachhuber (1971), major species of vegetation found in this area are Sporobolus airoides (drop seed), Oryzopsis hymenoides (Indian rice grass), and Sitanion histrix (squirrel tail). On the topographically high gypsum/clay dunes, the soil is typically a ustgypsoorthid that is mapped as the Karde loam (Boulier and others,

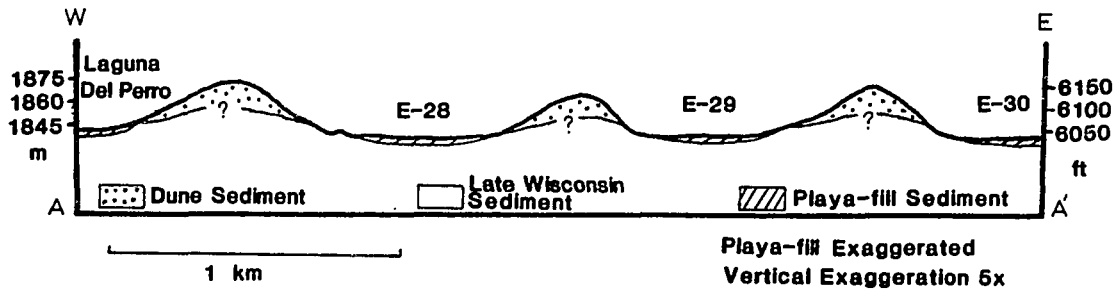
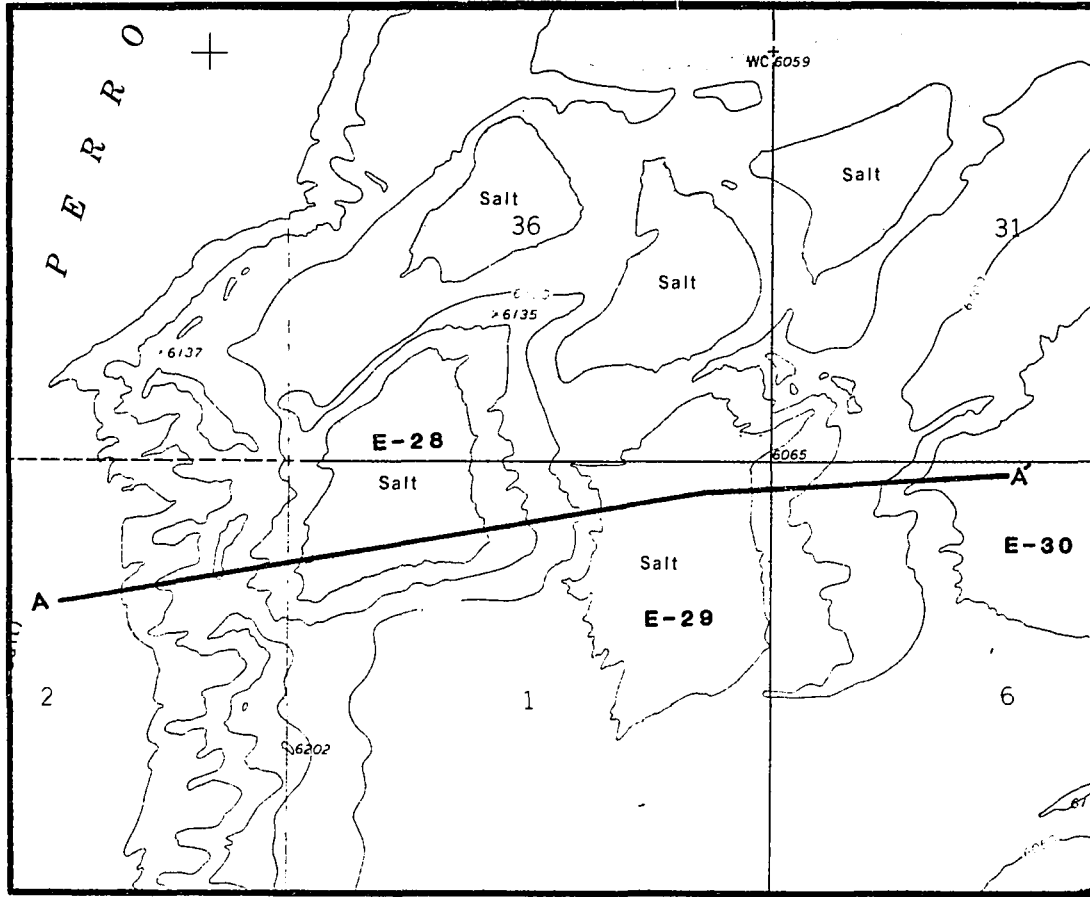


Figure 2. Plan view and east-west cross section showing topography through playa E-28, 29, and 30. Map from United States Geological Survey, Laguna Del Perro North 7.5' quadrangle.

1970), where Hilaria jamesii (galleta) and Butchloe dactyloides (buffalo grass) are dominant, favoring the sandy and more permeable soil. Finally, adjacent to the harshest environment in the basin, the playa floors, several saline-indicator species such as Allenrolfea occidentalis (iodine bush) and Suaeda suffrutescens (seepweed) are common.

Based on the amount of vegetation measured in numerous 30 m traverses, it is calculated that vegetation presently covers an average of 12% of the ground surface in the flat interdune areas, 9.5% of the dunes, 12.7% of the proposed earthflow scars, and only 5.7% of the steeper deflation-basin slopes. The interior of playas is void of vegetation.

### **Climate**

The Estancia valley is an isolated basin in the orographic shadow of the Manzano and Sandia mountains. Climate within the valley ranges from an arid to semi-arid valley floor to the more temperate sub-humid conditions of the valley slopes.

Rainfall that reaches the Estancia Valley is seasonally convective or cyclonic. From October to April, rains are derived from eastward moving Pacific frontal air masses. These rains are generally of low intensity and high frequency. From April to October, the rains result from convective air masses moving north from the Gulf of Mexico and are more intense, sporadic, and localized (Gabler and others, 1982). The mean annual precipitation for the town of Estancia (elevation 1,863 m) between the years 1904 to 1960 is 31.29 cm. Of this, 20.92 cm (67%) falls between April and September and half of that occurs during July and August. The mean annual temperature for Estancia, based on a 43 year period, is 10 degrees C with an annual mean maximum and minimum of 20 degrees C and 0.3 degrees C respectively.

At the higher elevations, the convectional systems are less pronounced and rainfall is generally more frequent and of low intensity (Gabler and others, 1982; Leopold, 1951).

The difference in precipitation between the central valley and higher elevations is documented at two other stations. At the town of Tajique (2,166 m) located 19 km west of Estancia and 305 m higher, a 41 year record documents a mean annual precipitation of 47.29 cm with 29.39 cm occurring during the months of April to September, half of which occurs during July and August. The mean annual temperature for the same period is 8.5 degrees C with an annual mean maximum and minimum of 18 degrees C and 0.3 degrees C respectively.

In the highlands of the Sandia Mountains, a 7 year record further documents that a 1,090 m increase in elevation yields an increase in precipitation. At the Sandia station (3,256 m) the mean annual precipitation is 56.72 cm which is 18% higher than Tajique and 45% higher than Estancia.

## **GEOLOGIC SETTING**

The geologic history of the valley is subdivided into five episodes of tectonic deformation that occurred during the: (1) Precambrian, (2) late Paleozoic, (3) late Cretaceous/early Tertiary (Laramide), (4) middle Tertiary, and (5) late Cenozoic (Woodward, 1982). The present regional topography is the result of late Cenozoic crustal extension that produced uplift of the Manzano and Sandia Mountains, formation of the Rio Grande Rift & the Estancia Valley, and development of the Jemez and Mount Taylor volcanic fields (Woodward, 1982).

Geographically, the Estancia Valley lies in the easternmost extension of the Basin and Range physiographic province and formed in response to late Cenozoic basin and range extension. The valley is closed structurally and physiographically. On the west, the valley has been downdropped against the

eastward dipping Manzano and Sandia mountains that rise to a maximum of 3,048 m. On the east, the valley is bounded by the Precambrian Pedernal Highlands, a narrow laramide-age plateau that reaches an elevation of 2,312 m, and their southern extension, the Rattlesnake Hills, at an elevation of 2,034 m. On the south, the valley is bounded by Paleozoic-age strata of the Juames and Chupadera mesas at elevations of 2,106 m and 2,220 m respectively. The north end of the valley is bounded by several isolated mountains containing the Ortiz porphyry belt, a middle Tertiary feature that stands at 2,500 to 2,700 m.

#### **Late Tertiary and Quaternary History**

Previous work within the basin focuses on the paleolimnology and biostratigraphy of the exposed Quaternary sediments (Bachhuber, 1971; 1982; Bachhuber and McClellan, 1977), geology and groundwater (Meinzer, 1911), Tertiary and Quaternary hydrogeology (Titus, 1969), paleoclimatology (Leopold, 1951; Antevs, 1954; Galloway, 1970; Brakenridge, 1978; Smith and Anderson, 1982), and archeology (Harbour, 1958; Lyons, 1969).

The stratigraphy of the valley is best summarized by Smith (1957) and Kelly (1972). Their work describes all of the stratigraphic units, however, a complete stratigraphic column is not exposed at any one area. Tertiary and younger units are generally considered as valley fill or pediment gravels, and are not defined as regional lithologies. It is suggested by Titus (1969), and Smith (1957), that these gravels or valley fill units originated in response to downdropping of the basin and are proposed to be correlative with the Pliocene Ogallala Formation.

With continued tectonic downwarping of the basin and increased alluvial activity, a thick sequence of valley-fill was deposited by early Quaternary time. Based on channels and bedded and nodular caliche horizons within the alluvium,

Titus (1969), believed that the basin had throughflowing drainage to the east and was subaerially exposed during the early Quaternary.

The earliest recognized Quaternary sediment in the Estancia fill is a 7 m sequence of clay. It is believed that the clay marks the first topographic closure of the valley. This material is thought to be Illinoian(?) in age and represents a pluvial interval referred to as Early Lake Estancia (Bachhuber, 1971) (Fig. 3). Overlying the Early Lake Estancia sediment is a 15 m thick sequence of interbedded sand, silt and clay. Titus (1969), refers to this sequence as the Medial Sand and he believes that it represents alluviation and eolian activity following the desiccation of Early Lake Estancia. Bachhuber (1988) recognizes the Medial Sand as an interpluvial deposit of Sangamon(?) age.

During early- to middle-Wisconsin time, alluvial deposition ceased and gradual accretion of paludal and saline-lacustrine deposits commenced (Bachhuber, 1982; 1987). These deposits of interbedded clays, silts, and gypsarenite, occur mainly in subcrop below the modern playa floor. The late Wisconsin section is exposed in the walls of the present deflation basins and documents glacio-pluvial conditions beginning at 24,300 yr B.P. (Bachhuber, 1987). This second major lake stand, Late Lake Estancia, is subdivided into a number of biostratigraphically distinct highwater and partial drawdown phases (Bachhuber, 1982).

Desiccation of Late Lake Estancia in the late Wisconsin, was followed by the development of the Estancia Playa Complex (Bachhuber, 1982). The Estancia Playa Complex, composed of interbedded red clays, silts, and gypsarenite, marks the onset of interpluvial conditions when the valley floor was subaerially exposed. Under latest Wisconsin climatic conditions, a final pluvial system, Lake Willard, expanded over the valley floor. A radiocarbon date from the Lake Willard section indicates highest lake level occurred at approximately

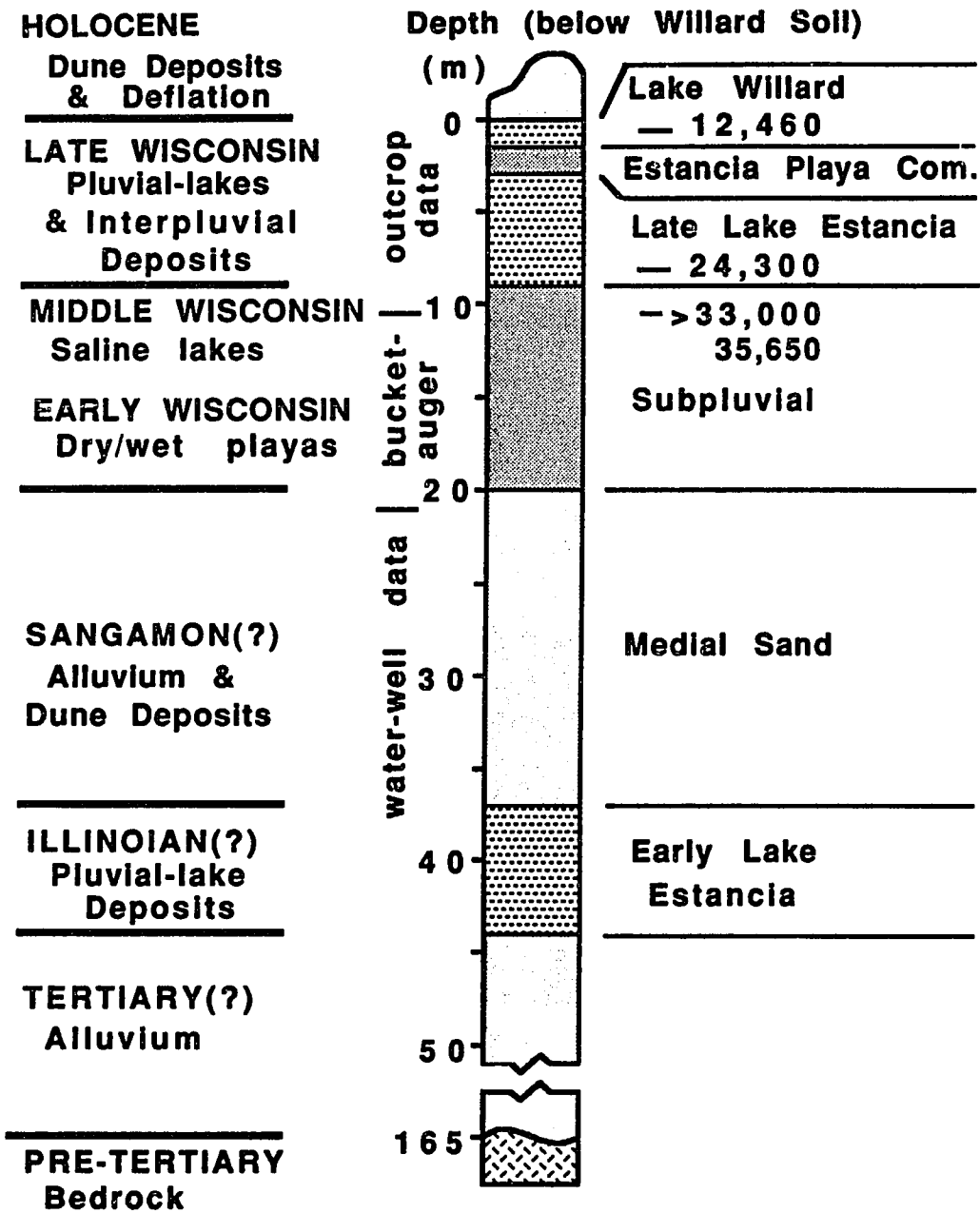


Figure 3. Generalized stratigraphic section of late Tertiary and Quaternary deposits in the Estancia Valley (After Bachhuber, unpublished figure).

12,460 yr B.P. (F.W. Bachhuber, personal communication, unpublished radiocarbon date). Overlying the Lake Willard clay is the Willard soil (Bachhuber, 1971). The Willard soil is an indurated gypsarenite that marks the desiccation of Lake Willard, the last major pluvial stand, and onset of the Holocene in the Estancia Valley.

The lithology of these sediments is important because the lacustrine clay and gypsarenite became major sedimentologic constituents of the clay/gypsum dunes and provided the shear plane for eventual earthflow movement.

#### **Early to Middle Holocene**

Formation of the Willard soil in the early(?) Holocene was followed by continued arid conditions that produced the first Holocene deflation/dune field, here termed the Meinzer Dune Complex (Fig. 4). The original extent and size of this dune field is unknown owing to what Bachhuber (1971) termed the Lake Meinzer interval, an inferred subpluvial event that temporarily flooded the inner basin. It is believed that wave action associated with Lake Meinzer eroded and modified the dune field producing the rounded and lenticular dunes seen today (Titus, 1969; Bachhuber, 1971). The lenticular topographic expression of the dunes, with barchanoid and transverse forms also occurring, are well rounded and stand at a maximum of 5 m high. The barchanoid and transverse dunes suggest later wind activity also modified these dunes.

Along the eastern margin of the playa complex, beach ridges composed of reworked dune material may be attributed to standing water from the Meinzer subpluvial event. There are also several modern deflation basins that expose poorly sorted, laminated, lacustrine(?) sediments (Bachhuber, 1971). These sediments suggest that the deflation basins of the Meinzer Dune Complex were infilled during the Meinzer subpluvial event and later exposed along the flanks of

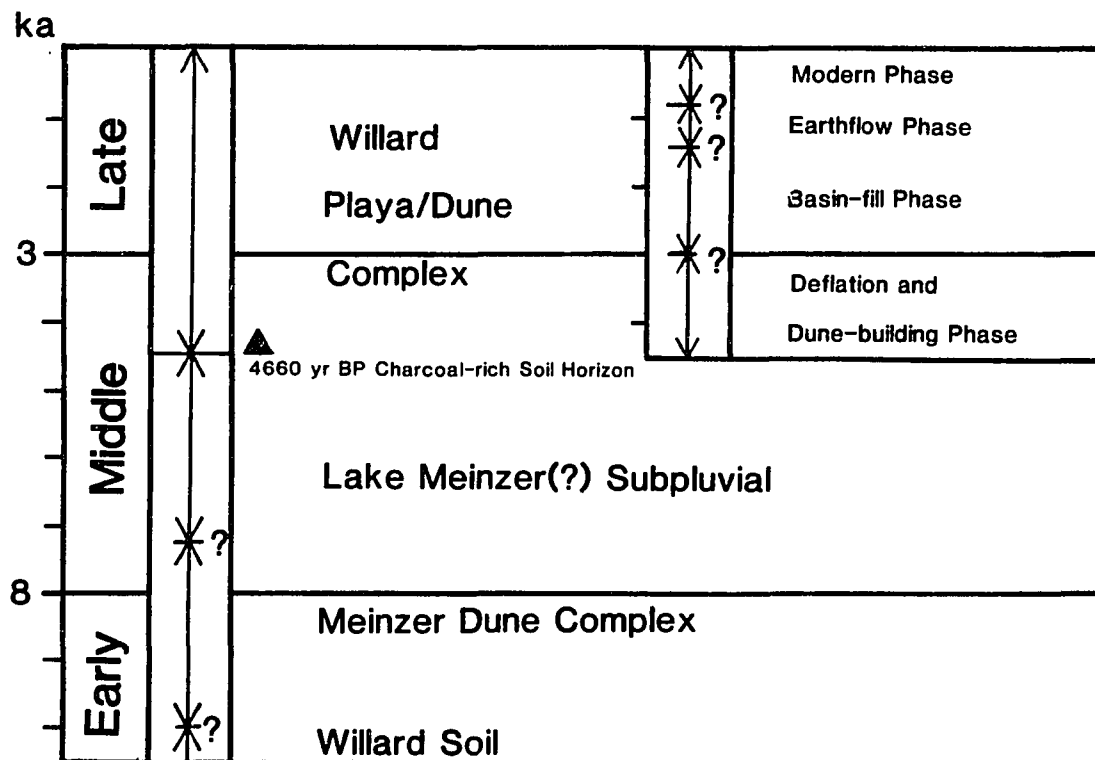


Figure 4. Holocene time table and the proposed middle and late Holocene chronology in the Estancia Valley. (ka dates after Spaulding, 1983).

some modern deflation basins.

### **Middle to Late Holocene**

The present deflation basin/dune complex, termed the Willard Playa Complex (Bachhuber, 1971), marks the end of the Meinzer subpluvial and a return to more xeric conditions. In exposed sections, dune material from this event is found covering the eroded lenticular dunes of the Meinzer Dune Complex. A radiocarbon date on a charcoal-rich soil horizon within the lower Willard Playa/Dune Complex deflation sediments, suggests that major deflation and dune development occurred in the late-middle Holocene after  $4,660 \pm 170$  yr B.P. (Fig. 5). Unfortunately, this date provides the only time constraint within the late Holocene. All the events emphasized in this study occurred after 4,660 yr B.P. and a more definitive chronology cannot be established at this time.

Evolution of the Willard Playa/Dune Complex is divided into four phases; deflation and dune building, basin filling, earthflow genesis, and modern degradation and aggradation which has significantly modified the size and shape of the deflation basins. Each of these phases will be discussed in detail later in the paper. Emphasis is on the earthflow phase which marks an interval of time depicted by the formation of mass-movement features.

### **SLOPE MOVEMENT PROCESSES AND EARTHFLAWS**

Elongated arcuate depressions, located on the in-facing duneslopes of deflation basins, are anomalous geomorphic features of the Willard Playa/Dune Complex. There are nearly 200 of these depressions which are typically 200 to 300 m long, 50 to 150 m wide, and are bounded by sharply-defined headwalls and lateral margins that generally represent 2 or 3 m of relief. The angle of the

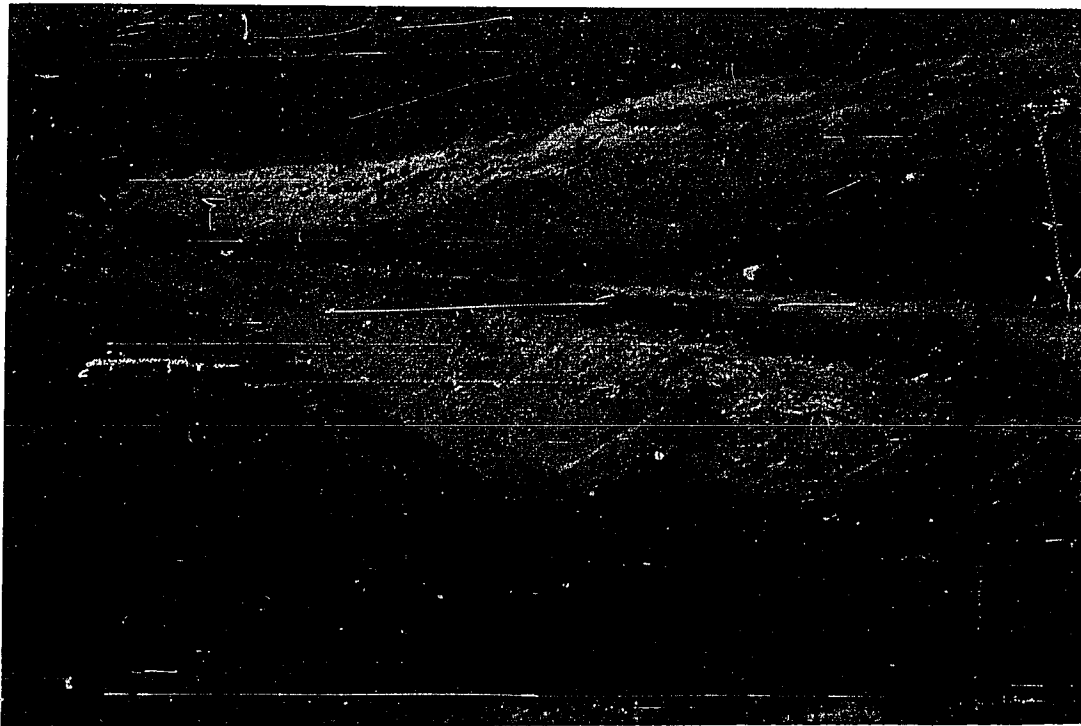


Figure 5. Exposure at E-28 revealing: edge of eroded Meinzer Dune (A), Willard Playa/Dune Complex parabolic-dune sediment (B), and dated soil horizon in lower Willard dune sediments (C). (Photograph by F.W. Bachhuber).

depression floors dip at approximately 5 degrees which is slightly less than the duneslope angle. The distal base of these features is truncated by modern playa expansion. These geomorphically striking features are thought to be relict earthflow scars.

## **SLOPE MOVEMENTS**

Landslide is a commonly used term that is applied to most types of slope-movement phenomena. This term is not accurate because it implies that a sliding mechanism is always involved. The term mass movement or slope movement, as suggested by Varnes (1978), is a more appropriately used and descriptive. Slope movements are typically short-lived, rapid-motion events that can be catastrophic in form, however, they can also be long-lived and move at rates of centimeters per year with either continuous or episodic motion. Slope movements, as noted by Coates (1977), are ubiquitous in most topographic regions and movement is commonly initiated or triggered by factors such as seismic activity, increased effective moisture, or the human factor.

There are numerous forms of slope movement which are defined by an interaction of variables. These include composition, grain size, mechanics (slide vs flow etc.), rate of movement, water content, and morphology. Based on these variables, numerous classification schemes for the different forms of slope movement have been proposed. These schemes often have an interdisciplinary bias and emphasize selected variables, therefore, no scheme has gained universal acceptance. The scheme proposed by Varnes (1978), is probably the most comprehensive and best summarizes the descriptive parameters of slope processes (Fig. 6).

A few of the studies that have gained universal acceptance in the field of slope stability include (Sharpe, 1939; Eckel, 1958; Zaruba and Mencl, 1969; and

TYPE OF MOVEMENT	T Y P E O F M A T E R I A L		
	BEDROCK	COARSE SEDIMENT	FINE SEDIMENT
FALLS	Rock Fall	Debris Fall	Earth Fall
TOPPLES	Rock Topple	Debris Topple	Earth Topple
ROTATIONAL SLIDES	Rock Slump	Debris Slump	Earth Slump
TRANSLATIONAL	Rock Slide	Debris Slide	Earth Slide
LATERAL SPREADS	Rock Spread	Debris Spread	Earth Spread
FLOWS	Rock Flow	Debris Flow	* Earthflow *
COMPLEX	Combination of two or more of the principal types of movement		

Figure 6. Abbreviated classification of slope-movement types (After Varnes, 1978). \* = proposed classification for scars of the Willard Playa/Dune Complex.

Schuster and Kriezek, 1978). Some of the first work recognized on earthflows was documented by Howe (1909) and Blackwelder (1912). Since slope movement has a different emphasis in different fields of study, there are many studies not listed here that are equally important.

### **Classification**

Earthflows are highly fluidized slope-movement processes that are composed predominantly of fine sand, silt, and clay-sized material. They behave as a viscous fluid, exhibiting random internal mixing and are differentiated from other types of slope-movement by particle size and mechanical properties. Based on the definition provided by Varnes (1978), the term "earth" refers to sediment in which 80% or more is finer grained than 2 mm in diameter.

Mudflows, which are commonly associated with earthflows, are generally less viscous, containing as much as 60% water and are exclusively silt and clay-sized particles. Debris flows are a much higher energy process, transporting poorly-sorted material that ranges from clay to boulder sized, half of which is greater than sand-sized.

Earthflow velocities vary from meters per year to meters per second. Keefer and Johnson (1983) document flows that move at rates of meters per day whereas rates of 26 km/hr and 300 to 450 m/minute have been proposed by Tavenas (1971) and Mitchell (1976), respectively. These rates of flow movement are certainly dependent upon several factors, most obviously the slope angle and viscosity of the flow material. The viscosity of flow material, which is related to the water content and composition, will vary for different earthflow complexes. Flows documented by Keefer and Johnson (1983) have water contents of 30 to 40% and exhibit slickensided-shear surfaces and irregular surface profiles; this suggests that the earthflows moved as a slow rigid mass. These flows, referred to

as "dry, slow earthflows", form in contrast to more fluidized "rapid earthflows" or "quick clay flows" that exhibit smooth surface profiles and distally deposited flow lobes (Varnes, 1978).

### **Morphology**

Typically, earthflow morphologies exhibit steep headscarps, distinct lateral margins, and gently sloping floors. The crown or headscarp is usually bowl shaped and can be tens of meters high and slope up to 90 degrees. The inclination of earthflow slopes ranges considerably, Keefer and Johnson (1983) note flows that occur on slopes between 8 and 45 degrees with most occurring between 20-25 degrees. Other workers document minimum slopes as low as 2 degrees.

Based on flow-scar measurements made by Mitchell and Markell (1974) and Mitchell (1976) in eastern Canada, the flow scar length ranges from 100 to 1,000 m and the ratio between the length of retrogression versus the original slope height (R/H) is typically greater than 10, but is most often between 20 and 80.

The outline of the flow scars vary from horseshoe, pear, tongue, and oblong shaped (Keefer and Johnson, 1983; Mollard, 1977). In gently dipping terrains, Mollard (1977) notes that flow scars often coalesce and that stepping, as a result of reactivation or from differing flow times, is common.

Morphologies for the zone of accumulation commonly terminate in a lobe or series of interfingering lobes that exhibit lateral ridges with slickensided shear surfaces and sinusoidal longitudinal profiles (Keefer and Johnson, 1983). In many cases, at the distal end of flow, the flow debris grades into the more liquid state of a mudflow and can cover an area of several square kilometers. Keefer and Johnson (1983) also note that rarely are flow masses deposited from a single

movement event, rather, they are built up over a period of years from remobilization of previous mass movement events.

Where associated with riparian conditions, these sediments are more conducive to erosion because sediments are quickly removed by fluvial processes and are less commonly preserved. In rare cases, Mollard (1977) documents pancake-shaped accumulation lobes. These lobes are best preserved where the sediment debris is deposited on level plains and is not subject to rapid removal by erosion.

### **Style of Motion**

Depending on the stratigraphy of the incipient flow sediment, earthflows can exhibit several different properties. Mitchell (1976) notes that if competent layers exist near the surface, they are useful indicators of flow mechanics. These layers are typically broken apart into blocks, which are rafted by plastic flow and/or liquefaction of the underlying soft sediment. The blocks usually show very little forward or backward rotational movement which is evidence for upper-layer translation as opposed to rotation. Near the headscarp, these blocks often drop or subside, producing a graben morphology.

Three phases of retrogression are believed to take place during flowage (Eden and Mitchell, 1973; Mitchell and Markell, 1974; and Mitchell, 1976). These phases are: (1) initial rotational slip failure, (2) retrogressive advancement of the headscarp, and (3) massive plastic extrusion.

### **INCREASED EFFECTIVE MOISTURE**

Although there are numerous factors involved in a slope stability problem, seismic activity and increased effective moisture are the most common attributes. Increased precipitation can destabilize an earth slope by increasing the load

(overburden pressure) and increasing pore-water pressure, subsequently displacing grain contacts and decreasing the resistance to flow (effective stress). These conditions of instability are augmented when there are contrasting hydraulic conductivity values within the sloping material (Coates, 1977).

If the Estancia features are the result of a climatically-induced mass-movement phenomena, then the variables discussed above, as well as the processes of destabilization, require consideration. Of primary concern is the role of loading and increased pore-water pressure.

### **Pore Pressures and Loading**

Under saturated conditions, pore-water pressure exerts an equal upward force in response to the total downward force (Huang, 1983). The downward force results from the mass of the material and any loaded components. Since water has a minimal compressibility factor, the greater the downward force applied, the greater the pore pressures (Morgenstern and Sangrey, 1978).

When assessing pore pressures, Morgenstern (1971), notes that the most important factor to consider is loading on the slope. Loading can result from the removal of a stabilizing factor, but most commonly results from the physical addition of mass to the unstable material, thus increasing the overburden pressure. The result of loading and increased pore-water pressure are especially critical when pore pressures cannot be dissipated due to low hydraulic conductivity of the material.

### **Hydraulic Conductivity**

Hydraulic conductivity is the measure of flow velocity through a porous media and is proportional to the hydraulic gradient (Freeze and Cherry, 1979). It also reflects the relative rate at which pore-water pressure can be dissipated.

Conditions of instability are enhanced when sediments that have relatively low hydraulic conductivity values lie beneath more pervious surficial material. These conditions can introduce high pore-water pressures at the interface of the two sediments, and if the overlying sediments also have relatively low hydraulic conductivity values, excess pore-water pressures can remain for an extended period of time. The occurrence of high pore-water pressures and low hydraulic conductivities are conducive to destabilization and liquidization.

### **Liquidization**

Under conditions of high pore-water pressure, the most significant factor pertaining to instability is the interaction between water and the composition of the material. This destabilizing interaction is described as liquidization (Allen, 1982; 1985). Liquidization is a process whereby a normally solid material changes state and behaves as a viscous fluid. Allen (1982), recognizes four types of liquidization; thixotropy, sensitivity, liquefaction, and fluidization. Thixotropy and sensitivity apply to cohesive materials and are conditions produced by a seismic event. Liquefaction and fluidization are applied to relatively non-cohesive materials and are conditions produced by loss of grain contact due to increased pore-water pressure or loading. The problem with this classification is that it disregards sediments that are both cohesive and granular.

Liquefaction results when pore-fluid pressure increases to a level that equals overburden pressure. The overburden weight is then supported by the pore-fluid pressure and the grains are entrained freely within the pore fluid. At this time, the sediment behaves as a viscous fluid (Owen, 1987; Allen, 1985).

### **MECHANICAL STRENGTH PROPERTIES**

The mechanical properties of an earthflow event are complex and involve

a host of variables. Understanding the role of these variables is essential when assessing a slope stability problem. The goal of this section is to determine the basic mechanical properties that constrain an earthflow event.

### Mohr-Coulomb Criterion

The most common way of determining the parameters of a slope stability problem is the Mohr-Coulomb criterion. The Mohr-Coulomb criterion is an equation that is used to determine the factor of safety for a particular slope. A factor of safety is the ratio between the resisting and driving forces and any value of one or less implies failure (Chowdury, 1978). Based on a known factor of safety of one or less, several of the variables constraining the earthflows can be estimated.

For a planar surface, the simplest mechanical model to represent slope stability consists of a mass on an inclined plane. The weight of the mass, or the normal force, produces a component of shear stress, and shear resistance at the interface. From Morgenstern (1971):

where  $\alpha$  = angle of inclination  
 $S$  = shear stress  
 $R$  = shear resistance  
 $W$  = weight

$$S = W \sin \alpha \quad \text{and} \quad R = W \cos \alpha$$

Since the interface is not frictionless, a frictional component that compliments the shear resistance, produces a total shear resistance or the shear strength, and is represented by:

$ST$  = shear strength,

$$ST = W \cos \alpha \tan \alpha \quad \text{or} \quad ST = R \tan \alpha$$

Furthermore, cohesion ( $c$ ) of the material is added to give:

$$ST = c + R \tan \alpha$$

This equation is adequate when instability conditions are derived in the absence of water. This is rarely the case, however, and the concept of effective stress needs to be employed.

### Effective Stress

Total stress analysis, as formulated above, is ideal for a situation where water does not affect stability. In most slope stability problems, a water pressure ( $p$ ) acts on the interface between the flow material and the underlying sediments. This pore-water pressure decreases the shear strength and destabilizes the mass. The resulting shear strength is referred to as effective stress. In a case where pore-water pressure is less than the shear resistance or near zero, effective stress can be estimated by subtracting pore pressure from the total shear resistance. Conversely, in a case where pore water pressure increases to equal the shear resistance, effective stress is zero and shear strength is a function of cohesion.

By applying the Mohr-Coulomb criterion for shear strength, the effective stress is represented by:

$$ST = c + (R \tan \alpha) - p$$

If the factor of safety equals shear strength divided by shear stress, then the final equation is:

$$F = \frac{c + (R \tan \alpha) - p}{W \sin \alpha} = \frac{ST}{S}$$

## **EARTHFLOWS OF THE WILLARD PLAYA/DUNE COMPLEX**

Based on the similar geomorphic preservation, there are nearly 200 suspect earthflow scars of the Willard Playa/Dune Complex that are believed to be relatively similar in age. Morphologically, these features are distinctively similar to the scars described previously for modern earthflows. Headscarps, lateral margins, and outlines greatly resemble known earthflow morphologies. In addition, because the sediment contains a high clay content and is easily erodable, the fresh appearance of the scars indicate their age is relatively recent.

I have divided the proposed Willard Playa/Dune Complex earthflows scars into three categories; slightly modified, modified, and greatly modified, type 1, 2, and 3 respectively (Plate 1). Criteria for subdivision are based primarily on post-flow erosion of the earthflow scar. Discerning differences between the type 1 and 2 scars is somewhat arbitrary, but the type 3 flow scars are distinctly more well defined and are probably the most recent. At playa E-28, all three states of preservation are present (Fig. 7).

### **LITHOLOGY OF THE EARTHFLOW SEDIMENT**

The earthflow scars occur in dunes composed of clay pellets and gypsum grains that range in size from clay to medium-grained sand. Based on gross percentage estimation in thin section, gypsum comprises 30 to 50% of the dune material. The gypsum grains range in size from several millimeters to clay-sized particles, and occur as fragmented and unfragmented lensoidal crystals that often contain opaque inclusions. The clay comprises 50 to 70% of the dune material and occurs as thin platelets and pellets up to several millimeters in diameter (Fig. 8).

X-ray diffraction analyses were completed at the University of Nevada,

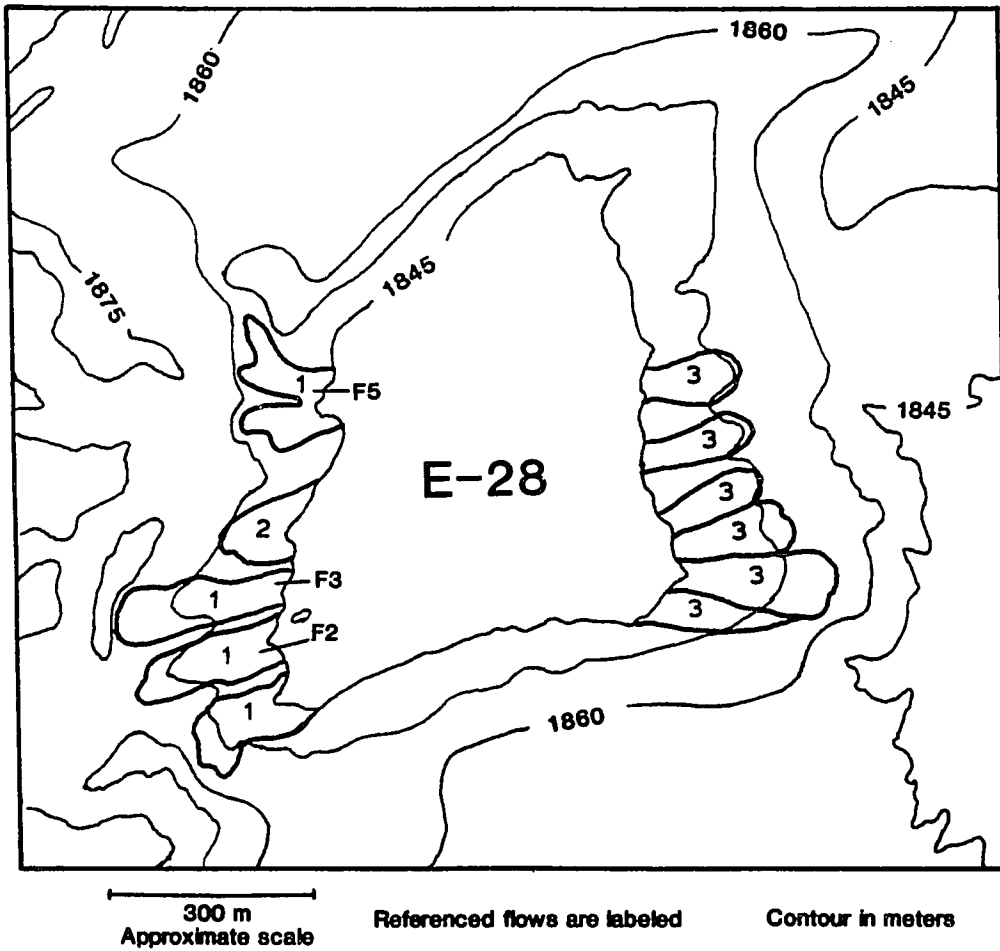


Figure 7. Slightly modified, modified, and greatly modified flow scars, type 1, 2, and 3 respectively, exhibited at playa E-28.

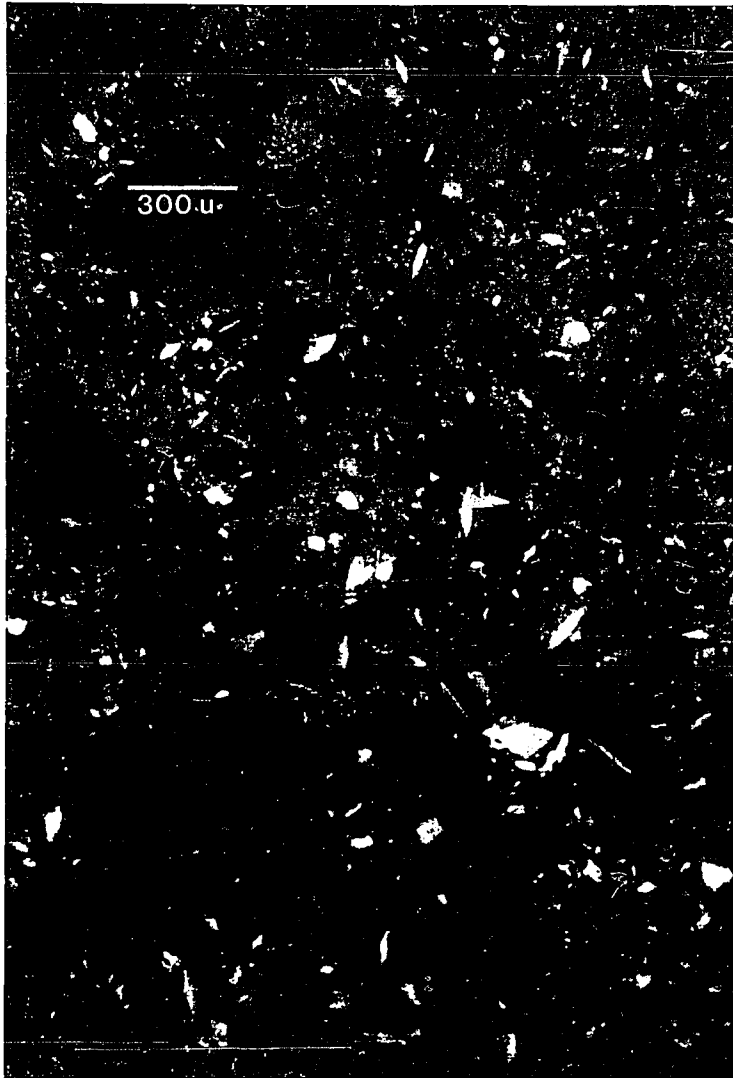


Figure 8. Photomicrograph of typical clay (brown) and gypsum (white) earthflow sediment.

Las Vegas. X-ray patterns strongly indicate that the clay is illite and kaolinite. Suspected peaks of illite become more intense, and kaolinite peaks become amorphous upon heating. Whole mineral tracings indicate a strong presence of gypsum, with calcite and quartz suspected to occur within the clay.

Major oxide geochemistry analyses were completed by Chemex Labs Ltd. in Sparks, Nevada (Appendix 1). These data support the X-ray diffraction data, revealing high concentrations of quartz, calcium oxide as gypsum and calcium carbonate, sulphate as gypsum, and carbon dioxide as calcium carbonate.

### **Origin of Sediments**

Gypsum in the Holocene-age dune material is derived from deflation of the underlying late Wisconsin interpluvial and pluvial sediments. The lensoidal gypsum crystals are believed to have precipitated initially in water-saturated playa sediment or in basin-margin clays during recessional pluvial phases. The crystals were probably reworked into basin-margin-dune material and littoral sands during interpluvial as well as pluvial episodes. The gypsum was subsequently washed back into the basin as gypsarenites where they often occur interbedded with profundal clays. The process occurs today as modern-dune material is transported back into playas.

Kaolinite and illite in the dune sediments are also derived from deflation of the lacustrine sediments. A lacustrine origin is supported by ostracodes found within the clay pellets. Both clay types were deposited during pluvial episodes of the late Wisconsin. Kaolinite, an aluminum silicate, and illite, a potassium aluminum silicate, are two and three layer clays respectively. Kaolinite formation is most commonly associated with felsic parent rocks and forms in an acidic environment. It is derived through hydrolysis, a primary weathering process, from potassium-rich feldspars or other silicates. Illite is also believed to be

derived from acidic parent rocks and the weathering of feldspars and silicates. However, illite most commonly occurs in an alkaline environment as a secondary clay, derived from diagenesis and alteration of other clay minerals or potassium-rich sediments (Deer and others, 1982). I suspect that kaolinite was the primary mineral produced during Pleistocene pluvial conditions and illite has, as suggested, formed as a secondary clay from the diagenesis of kaolinite and the present alkaline environment. Velde and Meunier (1987), however, document formation of primary illite at orthoclase-muscovite boundaries which suggests that illite may also be derived in situ, as a primary clay.

## **GEOMORPHIC EVIDENCE**

The earthflow scars of the Willard Playa/Dune Complex are in various states of preservation. Although different stages of geomorphic preservation are delineated, their overall similar morphology indicates that they formed during a relatively short and distinct time interval. In the most well preserved cases, headscarps, sidewalls, and gently sloping floors are distinct. In the more eroded cases, these features are poorly defined and often resemble deflation scours.

### **Morphology**

The arcuate-shaped scars of the Willard Playa/Dune Complex often exhibit well-defined headscarps with distinct lateral margins and gently sloping floors (Fig. 9). The headscarp crowns range from the common bowl shape to irregularly modified forms and are typically 2 to 3 m high. Most headscarps slope between 30 and 60 degrees, however, some are gradational with the floor of the flow and scarp height is interpretive. Sloping between 3 and 7 degrees, the floor of the scars are hummocky but structurally featureless with a smooth surface profile and lack ridges, cracks, or rafted blocks. This suggests that these were



Figure 9. Flow scars on west side of E-28 revealing headscarp and lateral margin morphologies. Note featureless, gently sloping floor. Scar in center of photo is E-28-F2 (see fig. 7). Also note ridge (A) and outlier (B) representing the depositional mode or zone of accumulation.

highly fluidized, rapid earthflows as compared to those described by Keefer and Johnson (1983) who document slower and "dryer" earthflows that exhibit rigid behavior and reveal slickensided lateral ridges.

The outline of the flow scars range from elongated semi-circles, horseshoe-shaped, and pear-shaped, to crudely dendritic with irregularly modified forms of all of the above. Many of the scars coalesce and are superimposed due to reactivation or slightly differing flow times.

Reactivation of some flows is evidenced by a lower set of sidewalls that occur within the perimeter of the main flow scarp. These scarps exhibit the same degree of preservation suggesting they formed shortly after initial flowage (Fig. 10). These secondary scarps should not be confused with the headscarp that are also on the floor of the flows. There are often several sets of headscarp walls occurring on the lower 20 m of the scar floor that probably function as knickpoints during storm runoff into the modern deflation basins.

Lobes of flow sediment which typically comprise the zone of accumulation are completely absent, but some flow debris sediment from this zone is believed to be preserved in a few isolated localities. Absence of these flow lobes is the result of deflation and lateral expansion of the modern deflation basins into which the flow sediment was deposited.

Upper-layer translation, as defined earlier, probably was not an active process. The dune sediment is not cohesive enough to have rafted blocks, therefore, there is no evidence for this process. The entire volume of flow sediment is homogeneous without any competent layers and is typical of plastic flow and/or liquefacted sediment.

### **Morphometry**

Although post-flow erosion has reduced the length of many flow scars and



Figure 10. Reactivation scarp (A) indicating two episodes of flow or remobilization on west-facing flow E-13-F4. Flow contact revealing load structures is below (Photograph by F.W. Bachhuber).

modified some morphologic features, most morphometric measurements were still readily attainable. Values for each of the scars vary and a general range of the values have been observed. Five basic measurements were made: (1) inclination or slope of the flow scar floor; (2) length of scar from headwall to playa margin; (3) width between lateral margins; (4) relief from floor of the scar to adjacent ridge; (5) angle of headscarps and lateral margins; and (6) R/H ratio. It should be noted that the retrogression versus slope height ratio is relatively low, ranging from 7 to 14 with most values centering at 10. This is a function of the dune crest to playa floor distance, which limits the length retrogression can advance. The preceding measurements for seven earthflow scars were obtained in the field, and additional measurements compiled from aerial photographs (Table 1).

### **Stages of Preservation**

The best preserved, type 1 earthflow scars are found at playa E-28 (Plate 1; Fig. 7) on the east side of Laguna del Perro. The scars are located on the east-facing slope of the deflation basin and exhibit clearly defined head scarps and lateral margins (Fig. 11). The margin of the playa basin truncates the flow scars and only the upper two thirds of the features are preserved. Two ridges extending out along the edge of the earthflow scars, contain a preserved extension of the earthflow debris.

Type 2 earthflow scars occur throughout the complex and exhibit similar morphologies but are not as well preserved. Head scarps are fairly well defined, but lateral margins are not distinct. The floor of most scars ranges from several degrees inclination to horizontal and are cut by arroyos. The arroyos, which tend to follow the axis of the scar drainages, typically cut steep-sided gullies into the base of the earthflow scar.

Flowskar	Length (m)	Width (m)	Slope Angle (degrees)	Lateral Margin and Headscarp Angle(degrees)	Depth of Scar (m)	R/H
E-28-F2	206	68	4-7	15-40	3-5	7.5
E-29-F3	223	63	4-7	15-40	3-5	7.3
E-28-F5	198	75	5-8	25-40	2-3	10.8
E-25-F2	330	165	2-3	15-30	4-7	13.5
E-25-F3	295	132	2-4	15-30	4-6	10.8
E-13-F4	340	130	3-7	15-40	3-6	11.1
LP-F2N	300	75	2-6	20-40	4-7	10.9

Table 1. Morphometric measurements of representative Willard Playa/Dune Complex earthflow scars.

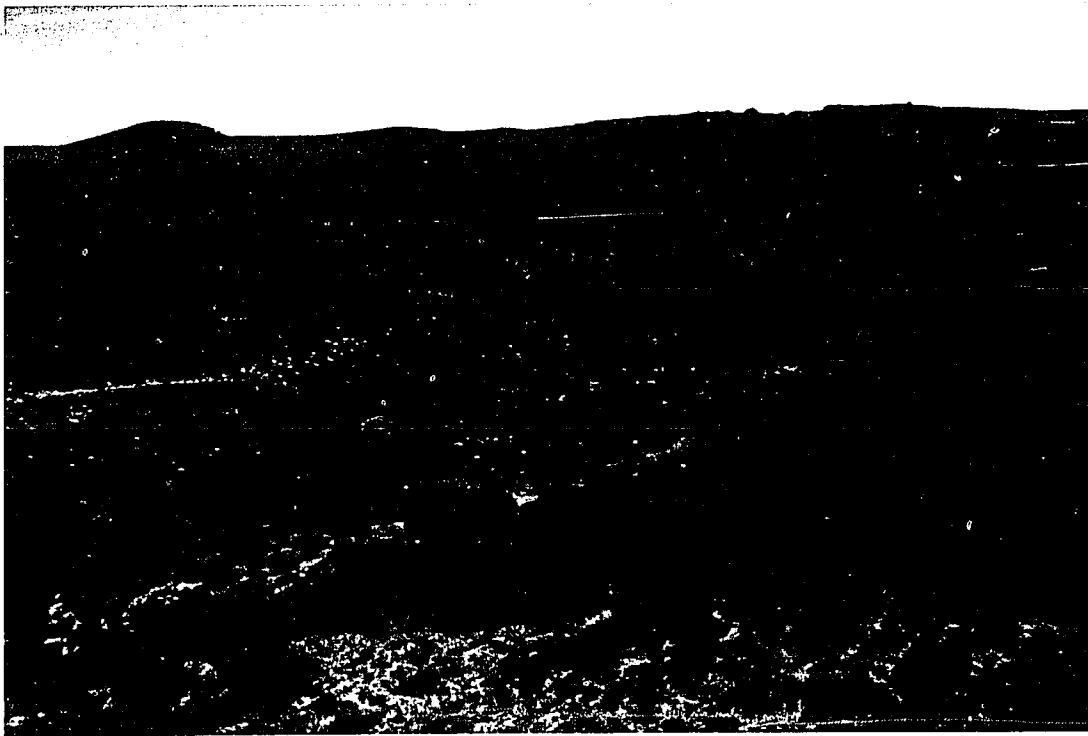


Figure 11. E-28-F5 (see fig. 7) a type 1 earthflow scar on the east-facing slope of playa E-28. Note well-preserved headwall, sidewalls and gently sloping floor.

In contrast to the type 1 flow scars, there are numerous examples of poorly-preserved earthflow scars that do not exhibit the classic features noted previously. These scars lack well-defined headscarps and lateral margins, and have also been extensively modified by fluvial and eolian activity. In one particular case along the west-facing slope of playa E-23 (Plate 1), these features exhibit low headscarps but lack sidewalls and a continuously sloping floor. The floor of these features slopes from the headwall, but becomes horizontal upon encountering more resistant sediments. These earthflows occur along modern deflation basins that are believed to be superimposed over probable basin-fill sediments from a pre-existing Meinzer Dune Complex deflation basin.

The differing states of preservation may reflect either multiple episodes of the flow event, reactivation, or may be a function of post-flow erosion. The overall similar geomorphic stage, however, as well as the large number of the earthflow scars throughout the complex, is suggestive of time synchronicity of the earthflow events, which in turn suggests a climatically- induced origin.

## **SEDIMENTARY EVIDENCE**

Along arroyos that expose the earthflow/lacustrine contact, sedimentary structures reflect evidence of erosional and depositional flow. The erosional mode, (zone of depletion) is one of high energy transport and exhibits rip-up clasts, flame structures, and modified channels. The depositional mode, (zone of accumulation) is a lower energy environment and exhibits convolute laminations and discontinuous bedding (Fig. 12).

### **Erosional-Flow Evidence**

The erosional mode, also called the zone of depletion by Varnes (1978), is preserved as the actual flow scar and represents the upper portion or main body

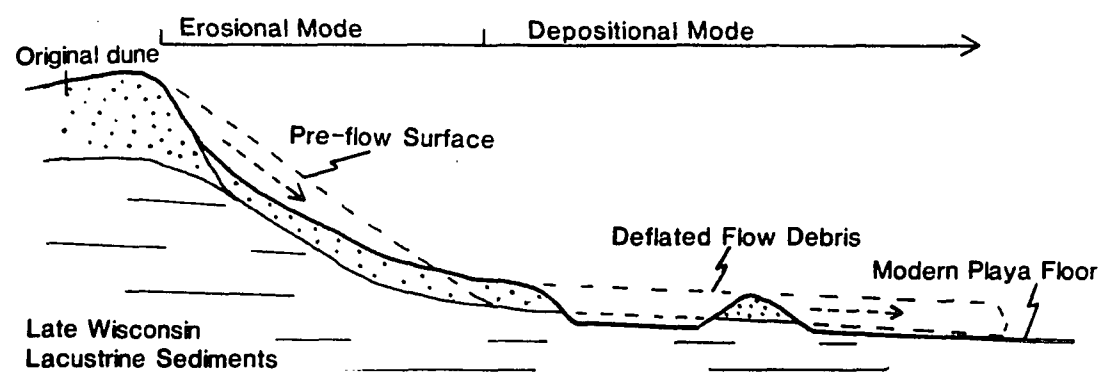


Figure 12. Diagrammatic cross section of E-28-F2 exhibiting erosional-flow evidence and depositional-flow evidence, the zones of depletion and accumulation, respectively.

of the flow that breaks away from the source. Erosional-flow evidence is typified by several types of sedimentary structures. The most diagnostic is rip-up clasts of lacustrine sediments that are entrained in the reworked dune material. These clasts, derived from the upslope, underlying lacustrine sediments, are texturally well preserved and range from rounded clasts of gypsarenite units to the subangular clasts of the interbedded siltstones and clays. The percentage of clasts ranges from a fraction to 40% within 50 cm above the contact.

Flamed-load structures also indicate erosional-flow evidence. These structures form on the surface of the lacustrine sediments, over which flow has occurred, and create a convoluted contact with the overlying reworked dune sediment (Fig. 13a). In an exposure on the west-facing slope of playa E-13-F4 (Plate 1), load structures are found in the lacustrine sediments that are overlain by flow material containing abundant rip-up clasts. The most impressive feature here is evidence of a load structure preserved as it was being sheared off and incorporated into the flow material (Fig. 13b).

Flame and load structures are produced by differential loading of the sediments when conditions of vertical anisotropy and rapid lateral density change occurs (Brodzikowski and Haluszczak, 1987). Based on descriptions by Kelling and Walton (1957), flame structures range from millimeters to centimeters in size and are longer in the vertical direction. The structures discussed here range from 5 to 15 cm high, with a broad base, and a slight elongation in the vertical direction. According to the proposed nomenclature for flame structures by Brodzikowski and Haluszczak (1987), these structures are considered large scale flame structures, more accurately described as flamed-load casts.

Formation of flamed-load casts developed when an earthflow mass moved down slope and adjustments for differential pressure and density were compensated for by the release or upward movement of sediment in a less

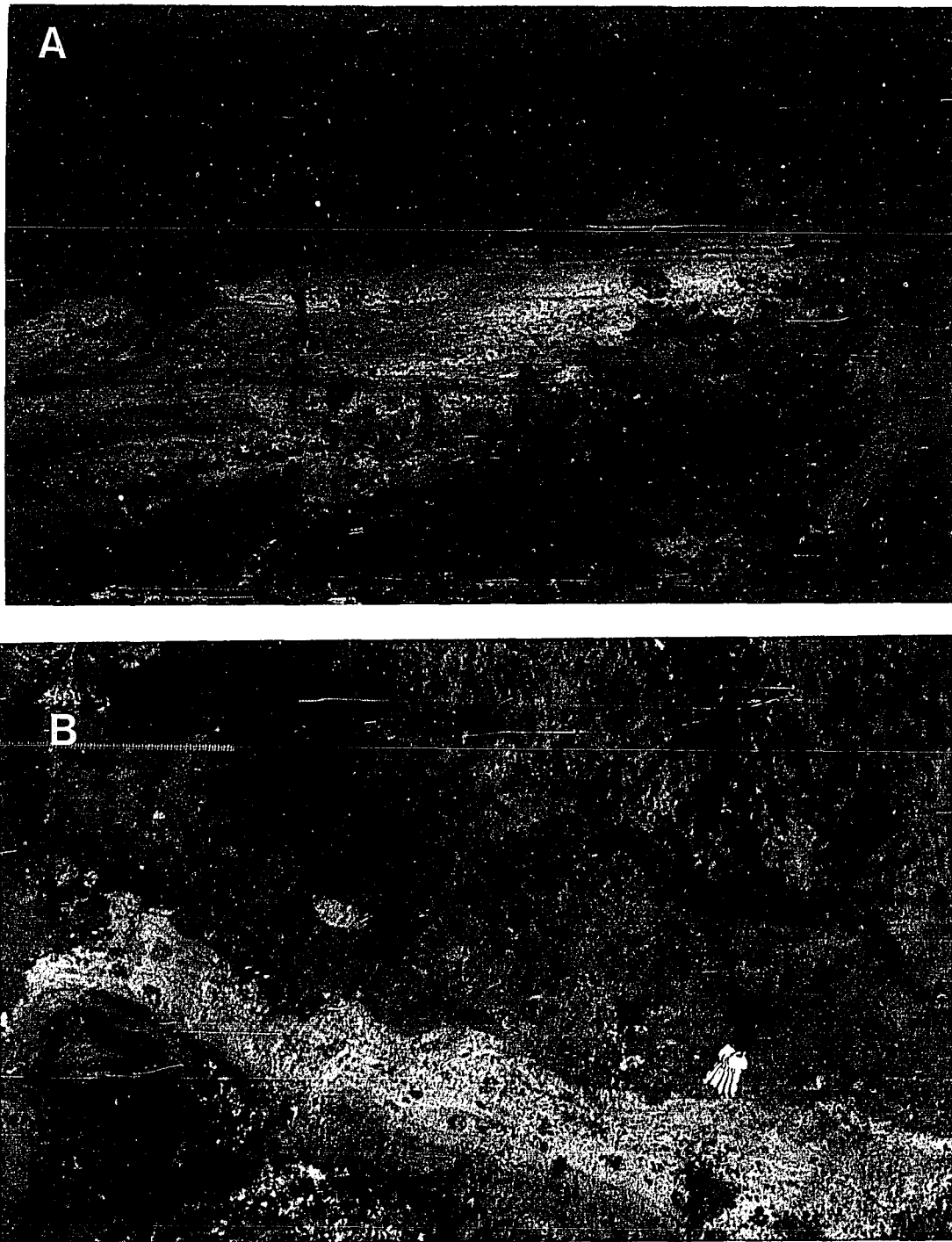


Figure 13. Erosional-flow evidence at E-13-F4. A: Flamed-load structures and smeared lacustrine sediments at the flow contact (motion is from right to left). B: Rip-up clasts of lacustrine sediment incorporated into the flow sediment (motion from left to right). Marker pen (14 cm long) and keys for scale.

competent or low pressure area. As the structure pushes up, it becomes oriented to reflect the directional component (Mills, 1982). The height of the structures and the sediment properties reflect the degree of differential loading. The stiff properties of the lacustrine sediments account for the broad structures.

A third form of evidence for erosional flow are the axial channels (Fig. 14). Although it is uncertain whether these channels were carved solely by the earthflow events or if they were pre-flow channels modified by flowage, field evidence argues for the latter. Based on the morphology of the flow scars, it is thought that a pre-existing structure controlled the flows. I believe that pre-flowage channels, acting as conduits for water, created conditions of high pore-water pressure and decreased effective stress, therefore inducing flow. Without the conduit that the channels provide, instability probably would have been laterally undefined. The channel dimensions were subsequently modified and enlarged by the flowage event.

### **Depositional-Flow Evidence**

The second type of sedimentary evidence for flow is found in the zone of accumulation and is referred to as depositional-flow evidence. These sediments are thought to represent the distal, low energy end of the earthflow where the material that was removed from the source area was deposited (Varnes, 1978). This evidence is less commonly preserved due to erosion and lateral expansion of the modern deflation basins and is best preserved along extended ridges and in an outlier sequence at playa E-28 (Fig. 15; Fig.12). These outcrops are extensions of the distal portion of flows and preserve fine convoluted laminations and discontinuous bedding. The laminations occur in the lower 30 cm directly above the lacustrine contact and are not continuous (Fig. 16a). Crude bedding of 1 to 10 cm thick clay-rich horizons are interbedded with poorly-sorted zones of

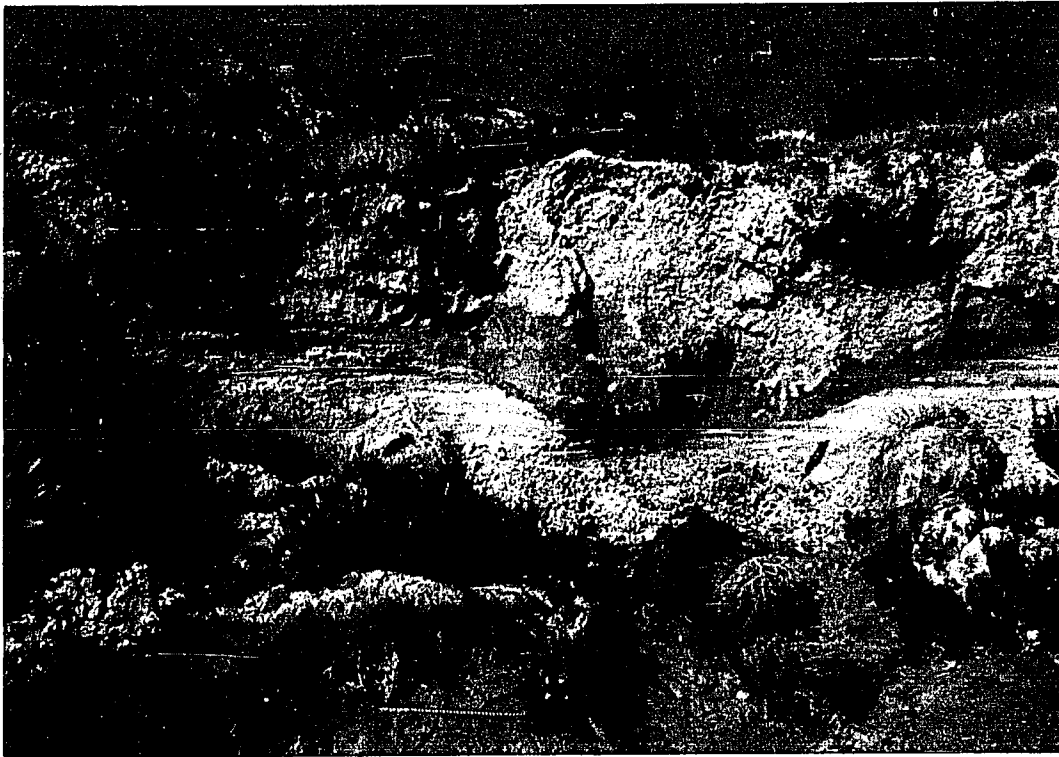


Figure 14. Flow material overlying channelized-flow contact. Exposure is in arroyo-cut headwall at E-28-F2 (see fig. 7). Pick-shovel handle approximately one-half meter.



Figure 15. Oblique view at Playa E-28 showing location of flow scars (A), preserved ridge (B), and outlier (C). Ridge and outlier preserve depositional-flow sediment (see fig. 9)(Photograph by F.W. Bachhuber).

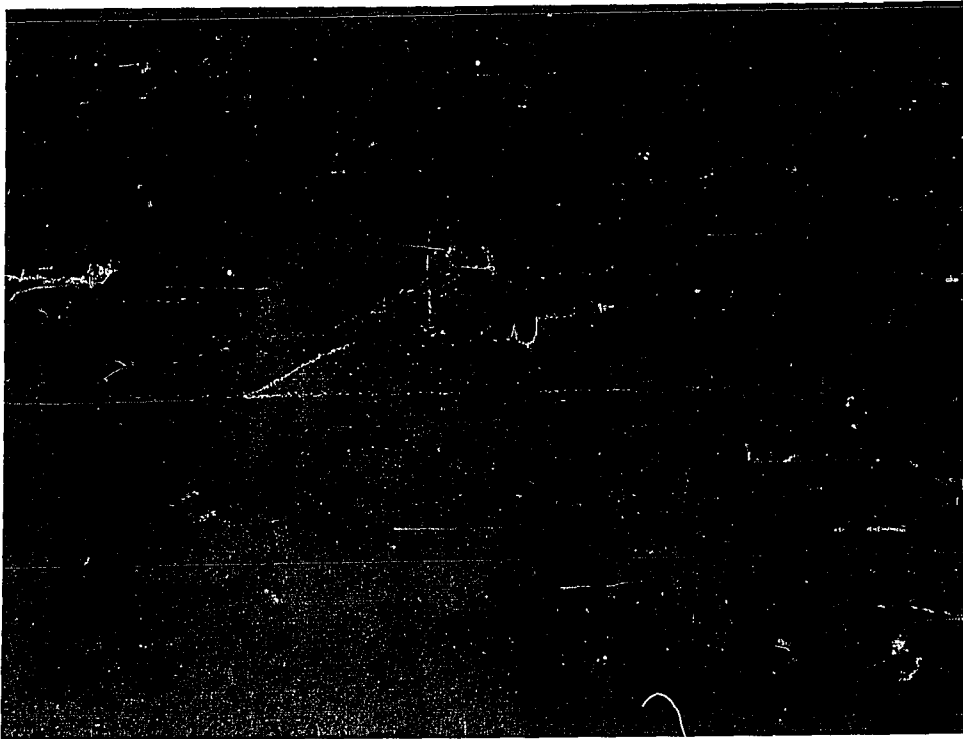


Figure 16. Depositional-flow evidence at E-28-F2. A: Trough and cross-laminated horizons above the contact. B: Continuous and uniform clay-rich horizons. Pick-shovel blade approximately 30 cm.

clay containing lithic and lacustrine clasts. Lithic clasts of basalt, quartzite, and gypsum are fine-sand to pebble sized and are derived from the lacustrine section. These poorly sorted units, containing lithic clasts, suggest turbulent flow and mixing at the proximal portion of the depositional mode.

On the playa floor of E-28, an outlier that stands 2 m high, 2 m wide, and 5 m long represents the most distal deposit of depositional flow yet located. Above the basinward-sloping contact, are several uniform and consistent beds of brown clay alternating with more gypsiferous units (Fig. 16b). The uniformity and fine-grained texture of these deposits is suggestive of laminar flow. At the time of flowage, it is likely that the deflation basins contained water and the lobes of water-lain earthflow sediment were disaggregated and dispersed over the basin floor.

### **PARTICLE SIZE ANALYSIS**

Grain-size analysis of bucket-auger and outcrop samples was completed by wet sieving all samples at the +1, +2, +3, +4, and +5 phi intervals. The material that passed through the +5 phi screen (< medium silt) was considered as the "pan fraction."

The samples were first analyzed prior to sieving to note any textural properties. After sieving, each fraction was analyzed for lithic fragments or other features indicative of flowage. Appendix 2 lists the results of sieve work.

### **Methodology**

Since most samples contain a high amount of pelletized clay, dry sieving does not indicate true texture of the sediment. Figure 17 compares a dry and wet sieve analysis for an identical sample of undisturbed dune (E-28-DC-2) sediment (Plate 1; Fig. 7). In the dry sieve analysis there is a distinct unimodal distribution

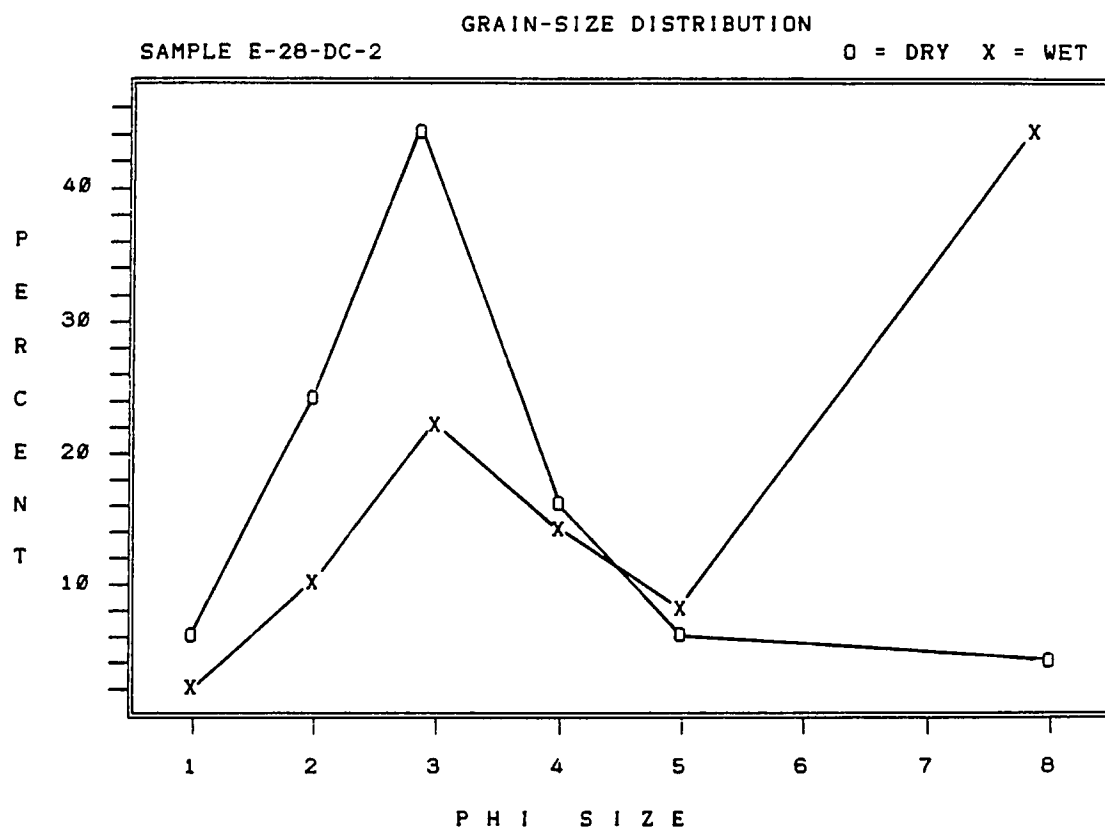


Figure 17. Comparative grain-size distribution for the same sample of undisturbed dune sediment when dry and wet sieved.

at the +3 phi size (fine sand), and in the wet sieve analysis, there is still a peak at +3 phi from the gypsum grains, however, a second peak develops below +5 phi (silt/clay range) due to disaggregation of the clay pellets. Even after treatment with sodium hexameta-phosphate and wet sieving, a portion of the clay-pellet matrix remains in the silt and fine-sand sized fractions.

### **E-28-F2 Bucket-Augered Borehole-Flow Samples**

At flow E-28-F2 (Plate 1; Fig. 7), bucket auger samples were extracted at 15, 55, and 110 m upslope from the deflation basin margin, holes 1, 2, and 3 respectively. Samples were taken every 0.5 to 0.75 m until the late Wisconsin lacustrine contact was encountered. Hole 1 and 2 encountered the contact at a shallow depth, with hole 2 encountering a 5:1 clay/silt to sand ratio 1.5 m above the contact. This clay-rich horizon may suggest mixing of the lacustrine sediments into the flow material. Hole 1 and 3, however, encountered a sharp lacustrine contact. Hole 3 reached the contact just prior to the end of the auger pipe at 9.0 m. Based on these contacts, the slope of the underlying lacustrine surface is inferred to dip at approximately 4-5 degrees; whereas the surface of the flow dips at approximately 5-7 degrees (Fig. 18).

A plot of the clay/silt to sand ratio for the three auger holes is based on the wet sieve results (Fig. 18). There are no anomalous trends between holes, and a 2:1 clay/silt to sand ratio is fairly consistent throughout the entire length of each hole. At the surface, it is apparent that clay is more concentrated (5:1 to 10:1) due to accumulation of fine sediment in the earthflow scar, and possibly by pedogenic processes.

### **Outcrop-Flow Samples**

Numerous samples were collected along arroyo cuts that expose flow

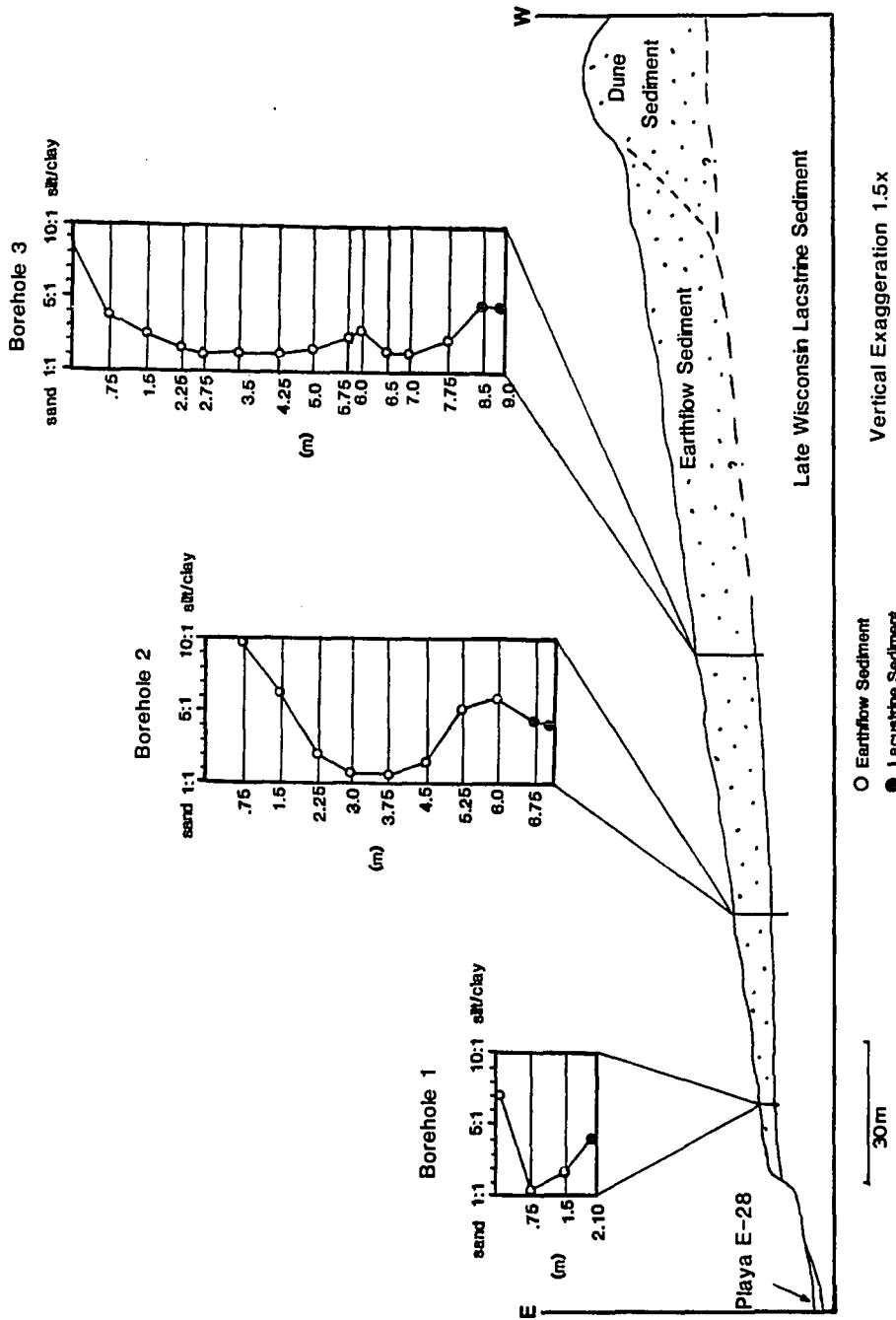


Figure 18. Longitudinal cross section of E-28-F2 (see fig. 7) revealing basal lacustrine contact and clay/silt (right) to sand (left) ratios for the three augered bore holes. Filled circles indicate lacustrine sediment.

material overlying the lacustrine sediments. At E-28-F2 (Plate 1; Fig. 7), samples FR-2, 3, and 4 were collected from a type 1 flow. FR-2 was taken in an arroyo cut headwall, 0.5 m above a channelized contact. At the same flow, FR-3 and 4 were collected 0.5 m above the contact along a ridge that is believed to preserve depositional flow evidence. With the exception of the +1 phi fraction (coarse sand), which is slightly higher in FR-2, all samples exhibit virtually the same size distribution. They have a bimodal distribution with a peak at +3 phi and greater than +5 phi. Slightly below FR-3 and 4, sample FR-5 was taken from a light-colored gypsiferous horizon that was slightly more indurated. This unit also exhibited a bimodal distribution, however, the peak at +3 phi shifted to +2 phi and became more platykurtic.

Although these samples do not exhibit any strong textural differences, the slight grain-size increase of FR-2 may reflect a gradual coarsening upward towards the erosional flow area. This would be consistent with the finely-laminated sediments found in the depositional flow area. The increased grain size of the FR-5 sample horizon reflects the increased gypsum content. This interbedded unit may result from a segregated sedimentation front. Sediment fronts occur during liquefaction and are described as an upward-moving restructuring event that separates zones of restored grain contacts below, from liquified "dispersion" zones above (Owen, 1987).

A ridge extending from an earthflow scar on the northwest corner of the playa (E-28-F5) also exhibits laminated horizons. At this location, there is a laminated pebble-rich unit of flow material that contains lithic fragments as well as fine pebble-sized gypsum crystals. These lithic fragments, which are derived from the lacustrine sediments, provide evidence that an earthflow mass incorporated these clasts from the up-slope underlying lacustrine section. Sieve results for this unit show a bimodal distribution with a platykurtic peak occurring

at +1 phi, and the typical clay/silt peak at greater than +5 phi.

At E-13-F4 (Plate 1), two samples were collected from flow material above flamed-load structures. Both samples exhibit the typical bimodal distribution, however, they have a very strong leptokurtic peak at +3 phi and a decreased peak intensity above +6 phi. Load structures, which form by upward adjustments due to unequal loading are commonly associated with a granular overburden where fluid pressures can escape more readily. The increased granular texture of these samples probably provided a more conducive medium for formation of the load structures.

#### **Sieve-analysis Summary**

Particle-size analysis of the earthflow sediment indicates a bimodal distribution near +3 and greater than +6 phi. These averages vary slightly, however, and samples taken above the contact, generally become skewed toward the coarse fraction at the erosional-flow area. The most anomalous sample occurred from sieve analysis of flow sediment above the contact at E-28-F5. This sample reveals lithic clasts in the small pebble-sized range that were derived from upslope, underlying lacustrine sediments.

In contrast to samples taken at the flow contact, the bulk of flow sediment, which occurs away from the contact, is texturally the same as the undisturbed dune sediment and reveals the same bimodal distribution.

#### **GEOHYDRAULIC CONDITIONS AFFECTING STABILITY**

Erosionally-truncated lacustrine sediments underlying unconsolidated dune sediments that are composed of 50 to 70% clay provided ideal conditions for slope instability. The addition of increased effective moisture accompanied by increased groundwater flow and a rise in the water table are believed to be the

primary triggers for instability of the Willard Playa/Dune Complex sediments.

### **Groundwater**

Water derived directly from increased precipitation is believed to have infiltrated and saturated the dune material while the increased groundwater flow into the central valley discharged at higher levels into the deflation basins. As a result of higher groundwater discharge, capillary water was drawn higher into the lacustrine sediments and overlying dune material. If groundwater flows were high enough, piping may have occurred. Piping results when heavy groundwater flow forces a conduit through the sediment to allow for greater discharge through the system (Mathewson, 1981; Coates, 1977). The primary effect of these conditions created high pore pressure at the interface of the dune and lacustrine contact.

### **Loading**

As a result of increased rainfall and the subsequent addition of more mass to the dune slope, it is believed that loading resulted in an increase in pore-water pressure and reciprocal decrease in effective stress. The increased pore-water pressure was especially critical due to the low hydraulic conductivity of the sediment which delayed dissipating excess pore pressures.

### **Pore Pressure**

At the dune/lacustrine interface there is a sharp contrast in the hydraulic properties of each sediment type. The dune material is coarser grained and more granular, whereas the lacustrine sediments are fine and massive. As a result of these properties, the dune material can dissipate pore-water pressures more readily than the underlying lacustrine sediments. The lower hydraulic

conductivity of the lacustrine sediments acts as a barrier, consequently, pore pressure at the lacustrine interface would be maximal and a slip plane would be provided.

Although the actual pore-water pressures are speculative, based on the Mohr-Coulomb equation, as pore-water pressure rises, the sum of the shear strength approaches zero. At the point when pore-water pressures equal shear strength, slope failure results. This concept suggests that these flows were induced by significantly high pore-water pressures that exceeded the weight of the mass, therefore the shear strength (numerator) was zero and cohesion was the only resisting force at the time of flowage.

### **Hydraulic Conductivity**

Experimental and theoretical values for hydraulic conductivity were measured using a falling head permeameter and the Fair-Hatch equation given by Freeze and Cherry (1979). Results for each are  $10^{-4}$  to  $10^{-6}$  cm/s and  $10^{-5}$  cm/s respectively. These values suggest that water passes through the dune material at a very slow rate, consequently, requiring rainfall of low intensity and long duration to become saturated. It also suggests that dissipation of high pore pressures due to a loading event would be very slow.

It should be noted that before the falling-head permeameter test was performed, a constant-head test was attempted. When the head was increased excessively, a piping affect resulted. This condition, as described earlier, suggests that piping and seepage erosion from increased groundwater flow may have occurred.

### **Clay-Water Interaction**

Although clay in the dune sediments was initially in the form of pellets

and relatively noncohesive, the pellets swell and disaggregate when wet, hence, the sediment becomes cohesive. I believe that the clay, upon losing its granular texture, acted as the fluid matrix and sustained pore pressure between gypsum grains. As a result of these conditions, the unstable mass of sloping dune material, that rested on more competent lacustrine sediments, was particularly conducive to mobilization.

### **Implications**

Because the earthflow scars of the Willard Playa/Dune Complex are relict features, the exact amount and duration of precipitation that induced flowage is speculative, nonetheless, some relative assignments can be made. Under present climatic conditions, the dune sediments are stable and undersaturated, receiving an average of 31.29 cm of rain per year. Two thirds of this (21 cm) occurs during the summer months and half of that (10.5 cm) occurs during July and August as a result of convective storm fronts.

These data indicate that even during a two month period of fairly high precipitation, the dune sediments are relatively unaffected and remain stable. This implies that the destabilizing threshold for the dune sediments and formation of the earthflows was not induced by short periods of intense precipitation; rather, they required continuous precipitation that fully saturated the sediments and caused instability.

Hydraulic conductivity measurements further support this, indicating that excessive intense precipitation would not infiltrate the dune sediment, but would function as runoff into the basins. Runoff occurs under modern climatic conditions and is responsible, in part, for lateral expansion and arroyo formation.

## ALTERNATIVE INTERPRETATIONS

Although evidence presented in this study strongly suggests that the arcuate-shaped scars are the result of an earthflow event induced from saturated conditions, there are two additional possibilities: (1) deflation scours, and (2) earthflows induced by a seismic event.

Well preserved headwalls and sidewalls can be delineated in the majority of the earthflow scars, however, many scars are heavily modified by secondary eolian erosion and do not exhibit the well preserved geomorphic features. These depressions resemble deflation scours on the windward-sloping dune material. Because depressions occur on all sides of deflation basins, it is unlikely that they were caused by erosion from a prevailing wind.

That the depressions resulted from earthflows induced by a seismic event, as opposed to being climatically induced, is also possible. Although there is no evidence of late Holocene faulting within the central valley, Machette (1982), documents Holocene faulting 35 km to the southwest. Because of the distance, however, it is questionable whether this fault impacted the central Estancia Valley. A plot of liquefaction due to seismic activity (Allen, 1985), suggests that, at 35 km, a seismic event of approximately 6.0 on the Richter scale would be required to trigger movement.

Northrop (1982), documents historical earthquakes in the Albuquerque area from 1893 to 1971. In a plot of quakes over 5 on the Modified Mercalli scale, there were no epicenters within or near the margin of the Estancia Valley. This is not necessarily the case throughout the late Holocene, but it is unlikely that a strong but distal quake would have triggered a flow event involving such a large number of spatially-controlled flows without the duneslopes already being destabilized and saturated.

## **HOLOCENE HISTORY AND DEVELOPMENT OF THE WILLARD PLAYA/DUNE COMPLEX**

The late-middle to late Holocene history and development of the Willard Playa/Dune Complex documents numerous climatic fluctuations in the Estancia Valley. These fluctuations, which include the proposed earthflow phase, suggest that the Estancia Valley record may hold implications for the regional setting of the late Holocene.

In the Estancia Valley, full-pluvial conditions were brought to a close with the desiccation of Lake Willard in the late Wisconsin and formation of the Willard soil in the early Holocene(?). The onset of xeric conditions resulted in the formation of the Willard soil and the first deflation basin and dune field, termed the Meinzer Dune Complex. Probable wave erosion associated with a proposed subpluvial event, referred to as Lake Meinzer, then eroded and modified the complex producing the current rounded dunes and possibly filling the original deflation basins with sediment. Termination of this wet phase brought about a period of quasi-stability evidenced by the formation of several soil horizons. These soil horizons, one of which produced a date of 4,660 yr B.P., mark the developmental onset of the Willard Playa/Dune Complex.

In this section, I will discuss the four developmental phases of the Willard Playa/Dune Complex. The discussion will include interpretive climatic factors and a description of the physical processes that provide evidence for each phase.

### **DEFLATION BASIN AND DUNE DEVELOPMENT PHASE**

This deflation phase documents a return to a more xeric climate following the Meinzer sub pluvial. At this time, deflation was the dominant process and was responsible for carving the large deflation basins into the late Wisconsin

lacustrine sediments. In addition to deflation, this phase marks a time of large dune formation and building that resulted in the parabolic dunes that occur adjacent to the deflation basins (Fig. 19a). Evidence of more recently active dunes as well as episodes of relative stability are noted by immature soil horizons within the dune sediment. The dunes, which attain a height of 40 m from playa floor to dune crest, dominate the landscape today.

At playa E-28 (Plate 1), 1 to 1.5 m of modern playa sediment overlies the original deflation surface. This sediment, which decreases at the basin margins, indicates that the floor of the basins were up to 1.5 m deeper than the present level. It is likely that decreased precipitation, being related to a hot, dry, and possibly windier climate occurred at this time and that a lower water table enabled deflation to remove the additional sediment.

A charcoal-rich soil horizon, dated at 4,660 yr B.P., occurs within the Willard Playa/Dune sediments, about 1 meter above the basal contact with an eroded Meinzer dune. This suggests that initiation of the Willard Playa/Dune Complex probably occurred in the late-middle Holocene after 4,660 yr B.P.

#### **DEFLATION BASIN-FILL PHASE**

In contrast to the conditions of the deflation and dune phase, the basin-fill phase represents a time when the energy regime shifted and erosion and deposition of the existing dune sediments back into the deflation basins prevailed (Fig. 19b). The primary mechanism that produced the change is likely to be increased precipitation. Evidence that supports the basin-filling phase is that many of the deflation basins have a thick ramp of reworked dune sediment overlying the original lacustrine-deflation ramp (Fig. 20). These sediments, which are stratified parallel to the basin slope, were formed when increased-precipitation events deposited the sediments in a basin-filling event.

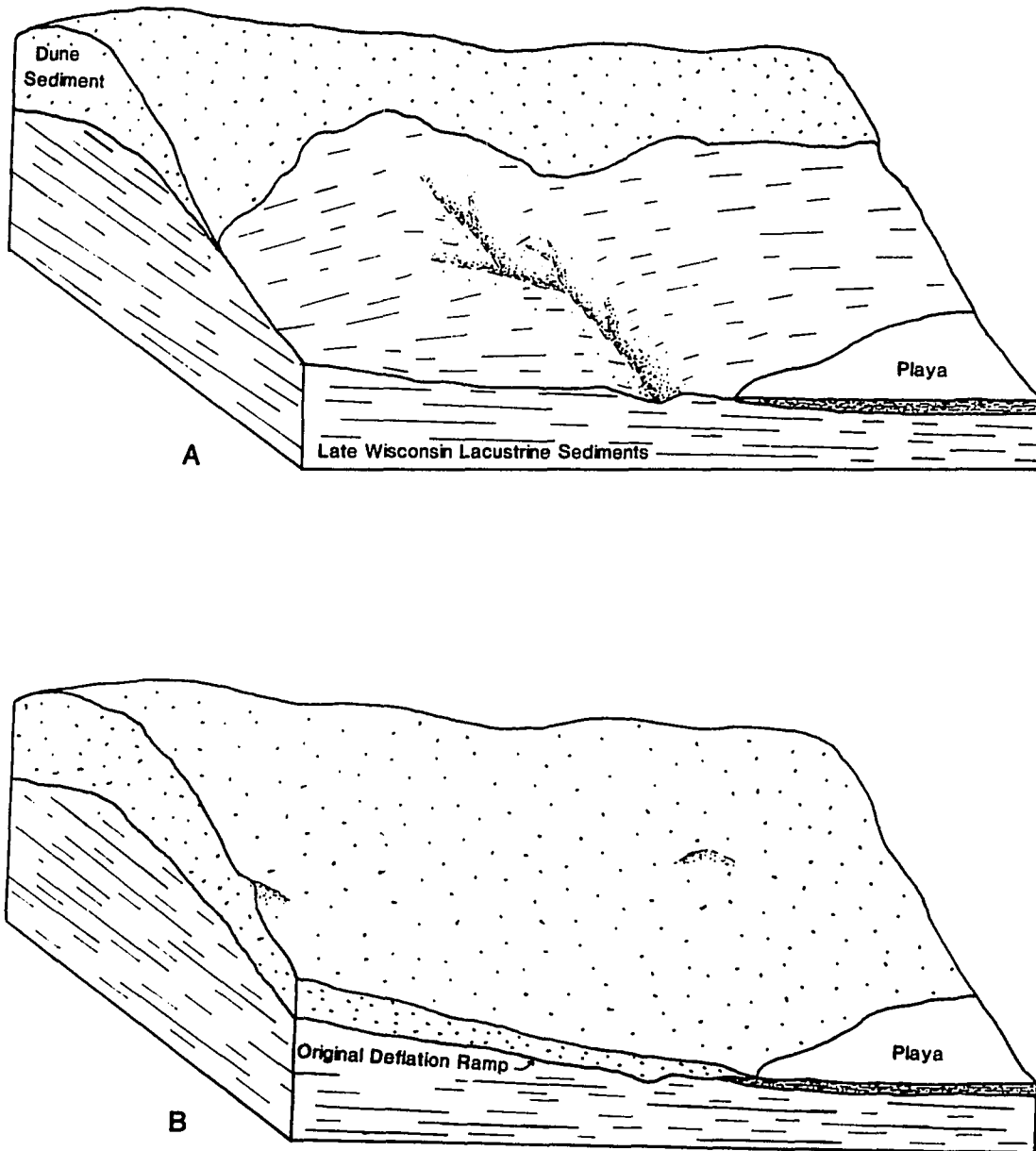


Figure 19. Deflation & dune-building phase (A), and basin-fill phase (B).  
 A: Note exposed ramp of lacustrine sediments and incipient flow channel. B:  
 Succession of sediment input and accumulation of reworked dune sediments on  
 lacustrine ramp.



Figure 20. Reworked basin-fill sediments (A) overlying lacustrine-deflation ramp (B) along east margin of E-28.

The sediments exhibit graded beds, some trough-cross bedding, and are locally calichified. Although basin-filling events are a continuous process, the thickness of these sediments found blanketing the sides of deflation basin margins, suggest that there was a distinct paleoclimatic phase typified by an increase in precipitation. This phase probably culminated in the succeeding earthflow phase.

### **EARTHFLOW PHASE**

Geomorphic and sedimentologic evidence supports the hypothesis that the earthflow phase marks the culmination of increased precipitation in the Willard Playa/Dune complex. This phase produced the large number of morphologically distinct scars found throughout the Willard Playa/Dune Complex (Fig. 21a). Although three different stages of preservation are recognized, the similarities bracketed by the greatest and least modified scars are distinct. Scars that are highly modified are well defined in general outline, but they do not exhibit sharp headscarps or lateral margins. Instead, the scarps are eroded and slope to form a gradual transition with the floor of the scars. The least modified scars exhibit distinct headscarps and lateral margins. They have, however, been subject to erosion, as there is little evidence for flow lobes other than isolated outcrops of flow debris. The absence of recent earthflows indicate that earthflow formation has not been a continuous process and similar preservation of the large number of earthflow scars suggests that they formed during a relatively short period of time.

Sedimentary structures found along exposed contacts between suspect flow material and the underlying lacustrine sediments indicate that the lacustrine sediments were deformed as a result of loading. In the zone of depletion, erosional-flow evidence reveals flamed-load structures and rip-up clasts indicating vertical anisotropy and a strong lateral component of motion.

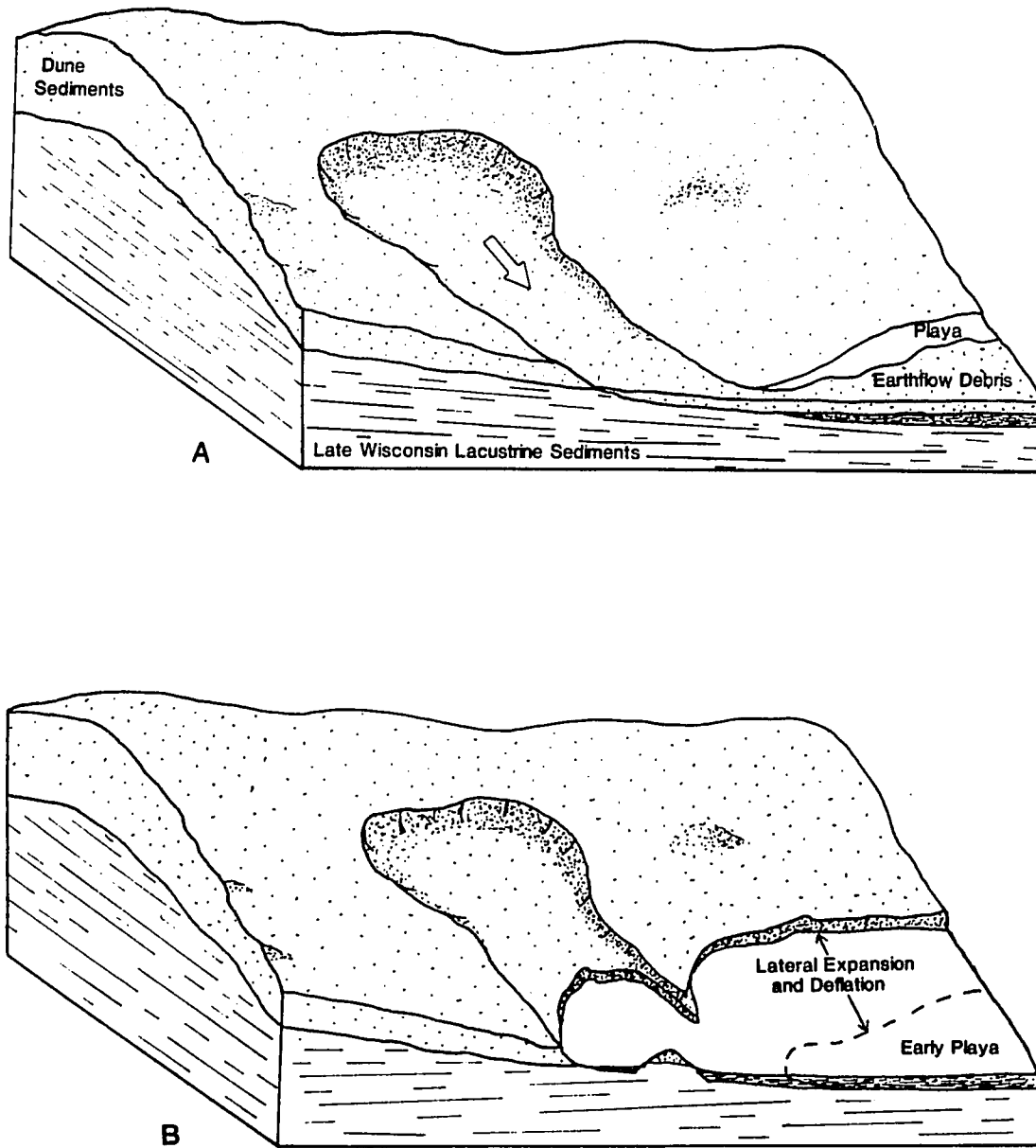


Figure 21. Earthflow phase (A) and modern phase (B). A: Note proposed distribution of earthflow debris in the zone of depositional-flow evidence. B: Removal of earthflow debris and most depositional-flow evidence.

Conversely, the zone of accumulation is almost completely removed and only isolated exposures reveal depositional-flow evidence. The flow lobes that comprised the zone of accumulation once covered most of the playa floor and have since been removed by deflation and lateral expansion of the basins (Fig 21b). It is also probable that the flows were initiated at a time when the deflation basins were partially filled with water. The resulting water-lain sediment was dispersed over the playa floor. This sediment cover was subsequently deflated during more xeric conditions when the water table beneath the playa floor dropped. If there was standing water in the basins, in addition to dispersing flow sediment over the playa floor, it is likely that wave erosion and the resultant removal of the toe added to instability and subsequent earthflow movement.

From the geomorphic and sedimentologic evidence presented, it is proposed that increased precipitation, infiltration, groundwater flow, and their interaction with the dune material, induced flowage by saturating and destabilizing the clay, as well as modifying the physical and hydrologic parameters of the dunes. The interaction between water and the clay within the dunes created conditions of high pore pressure, decreased effective stress and possibly caused liquefaction of the sediment.

In summary, there are several parameters believed responsible for slope instability and the earthflow event of the Willard Playa/Dune Complex. Primarily, loading that resulted from increased mass of the water-saturated dune sediments produced high pore-water pressures. These high pore-water pressures were not dissipated quickly due to low hydraulic conductivity of the sediments, thus creating slow-draining conditions. Furthermore, stiff lacustrine sediments at the base of the dune sediments created an even greater barrier for dissipating high pore-water pressures. This channelized and sloping interface provided a failure plane for unstable material that has low cohesive strength and is

susceptible to flow and or liquefaction. Finally, possible removal of the toe through wave action decreased shear strength and induced flow.

### **MODERN PHASE**

Precipitation patterns indicate that the modern climate of the Estancia Valley is presently influenced more by summer convectional precipitation than by winter storm fronts. Dominance of this system indicates a shift from the proposed higher frequency, lower intensity precipitation of the earthflow phase. The increased nonconvectional precipitation documented at higher elevations is also thought to affect the groundwater system of the lower valley. These modern climatic conditions are probably more xeric than the preceding earthflow and basin-fill phase, however, a higher water table and minor dune activity indicate that it is probably less xeric than the initial deflation and dune building phase.

As a direct result of modern climatic conditions, several processes are actively modifying the topography of the Willard Playa/Dune Complex. These active degradational and aggradational processes are identified as: (1) deflation of earthflow sediment, (2) arroyo cutting and slumping, (3) aggradation of the playa floor, and (4) lateral expansion and eolian activity.

#### **Deflation of Earthflow Sediments**

The most striking factor pertaining to the modern phase is the absence of earthflow debris; especially because the playa-floored deflation basins were probably blanketed by earthflow sediment at the close of the earthflow phase. Based on the amount of relief between the flow contact at an outlier and ridge at E-28, the minimum thickness of these sediments was about 2 meters. The subsequent removal of these flow sediments in the zone of accumulation, is attributed to deflation. If the volume of the scar represents the amount of

material that flowed onto the playa floor, then the volume of earthflow sediment can be approximated.

In an attempt to quantify this process, the areas for the zones of depletion were calculated with a polar planimeter and the thickness was based on an average relief value. Calculations indicate that 42,500 m<sup>3</sup> of flow sediment was removed at E-28-F2 and nearly 400,000 m<sup>3</sup> of flow sediment was removed from the entire E-28 deflation basin (Plate 1). All mapped earthflows within the Willard Playa/Dune Complex contributed approximately 8.2 million m<sup>3</sup> of sediment into respective playas, most of which has subsequently been removed by deflation.

These data imply that since the time of earthflow formation, a significant amount of sediment debris has been removed, and that eolian processes in the modern phase have been the dominating forces responsible for degradation of the Willard Playa/Dune Complex. Because recent dune formation is not much in evidence elsewhere in the complex, the final destination of this volume of deflated material may be outside the complex, however, this is unknown.

### **Arroyo Cutting**

Arroyos that result from surface runoff into the deflation basins are ubiquitous throughout the playa complex. Each deflation basin and associated duneslopes represent an individual drainage basin. The amount of water that is collected in any given drainage basin from direct precipitation is a function of basin size. The extent of arroyo development appears to reflect this factor with larger and deeper basins noted by a more extensive and entrenched arroyo system. Arroyos in the central complex, which are more pronounced due to large basin size, are steep sided and sinuous, extending as far as 20 m from the basin margin.

Although present total precipitation is believed to be less than that of the earthflow phase, the arroyos document episodes of high intensity, short-duration precipitation. The dune material, with high clay content and low hydraulic conductivity, has low infiltration rates, therefore, water derived from high intensity precipitation events is not quickly absorbed into the dune material and is more conducive to runoff and arroyo development.

Furthermore, as a result of the steep sided, entrenched arroyo cuts, large pillars are produced along the walls of arroyos. These pillars topple into the arroyos and are mass-wasted and washed onto the playa-floored deflation basin (Fig. 22). The process of dune degradation (i.e., runoff and arroyo cutting) leads to basin aggradation as sediment is carried onto the playa floor, however, the majority of it appears to be rapidly deflated.

### **Aggradation**

On the playa floor of the deflation basins, aggradation and degradation are active processes. Theoretically, aggradation occurs in the winter months when reduced temperatures decrease evaporation and the playa remains wet (i.e., the water table is at the surface). Degradation occurs in the hot summer months when the water table drops, the playa floor dries, and wind deflates the desiccated clay and gypsum. A paradox exists, however, in that the Estancia Valley has 67% of its precipitation occurring in the summer months, thus sediment input onto the playa should be greatest at this time.

Although deflation of the earthflow sediments suggests that deflation is the dominate modern process, the present accumulation of playa sediments is believed to be a function of a rising water table and is evidenced by a fairly uniform accumulation of clay and gypsiferous units. In addition, aprons of dune-alluvial sediment occur along the margins of deflation basins. These

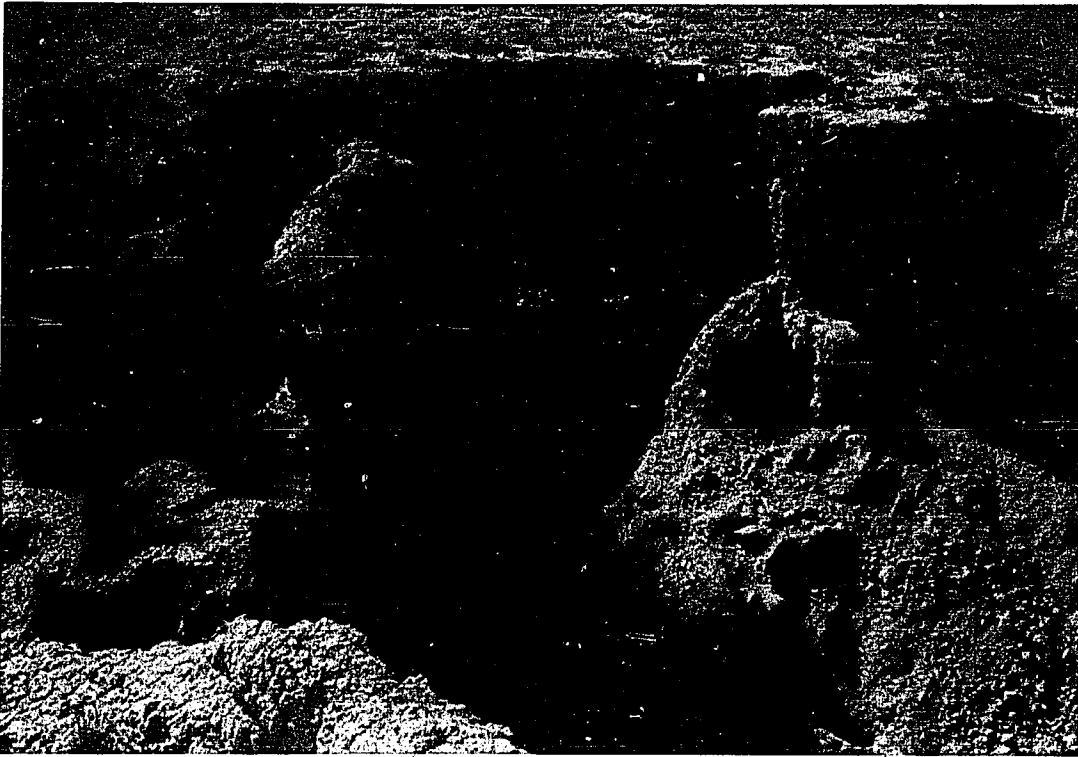


Figure 22. Topple-block columns at arroyo-cut headwall at north margin of E-23.

sediments form in response to degradation of the dunes during high intensity precipitation.

### **Lateral Expansion and Eolian Activity**

Lateral expansion, which is the outward erosion of the deflation basins, is seen in duneslopes that have been eroded back from the original margin of the playa floor. By extrapolating the non-eroded duneslopes into the basins, the original size of the deflation basins is approximately 30% smaller. The process of lateral expansion occurs in two ways, wave erosion and eolian activity.

Lateral expansion from wave erosion, which is more pronounced in the innermost deflation basins, results from higher groundwater levels with respect to the topographic level of the central basin. In periods of high precipitation, water in the lower, central complex, rises above the playa surface, subsequently, wind causes wave erosion of the deflation-basin margin.

If wave erosion and lateral expansion indicate that groundwater levels are relatively high, and if termination of the earthflow phase documents a decrease in effective moisture, it is probable that the deflation basins were partially filled with water at the time of the earthflows. Sediments revealing uniform and continuous laminations in the depositional mode support this idea.

Lateral expansion as a result of renewed eolian activity is also presently occurring in many of the deflation basins in the center of the complex. Corresponding to west-southwesterly winds, the most active areas occur along west-facing slopes and reflect two geomorphic stages. The first stage occurs as deflation on gentle slopes, producing hoodoos up to 1 m high. The second, more advanced stage of eolian activity, occurs in the northeast corner of deflation basins where a complete section of late Wisconsin lacustrine and Holocene eolian sediments have been exposed by deflation of the duneslope. These

exposures are steep sided and reveal approximately 10 m of the late Quaternary lacustrine section, and up to 15 or 20 m of the Willard Dune Complex sediments (Fig. 23). In more advanced stages, large wind-excavated blowouts or "amphitheaters" have been formed in the southeast or northeast corners.

Evidence of deflation basin piracy or joining is apparent at E-8, E-21, E-38, and Laguna Del Perro (Plate 1). Corresponding to southwesterly winds, growth direction of the basins is greatest in the northeast corners, subsequently, many of the basins are elongated in a northeast/southwest trend. Both, water and wind are believed to be responsible for lateral expansion and are currently modifying the topography and configuration of the modern deflation basins. In comparing aerial photographs from the 1940's to 1974, only one minor slump feature occurring during this time interval was detected. The dimension of the playas, even in the northeast corner where deflation is most active, reveal only minor changes.

## CONCLUSIONS

The relatively xeric deflation and dune building phase commenced with deflation of the lacustrine sediments and subsequent deposition of the associated dunes. The lowermost dune deposits from this phase contain a charcoal-rich soil horizon dated at 4,660 yr B.P.

The basin-fill phase, marks a time of increased precipitation and possible decreased wind velocities. Basin filling is seen in a thick sequence of dune sediment and local calichified zones overlying the slope of the deflated lacustrine sediment.

The nearly 200 arcuate-shaped scars that occur on in-facing duneslopes of the Willard Playa/Dune Complex are the result of slope instability and an earthflow event. This earthflow phase documents the culmination of increased

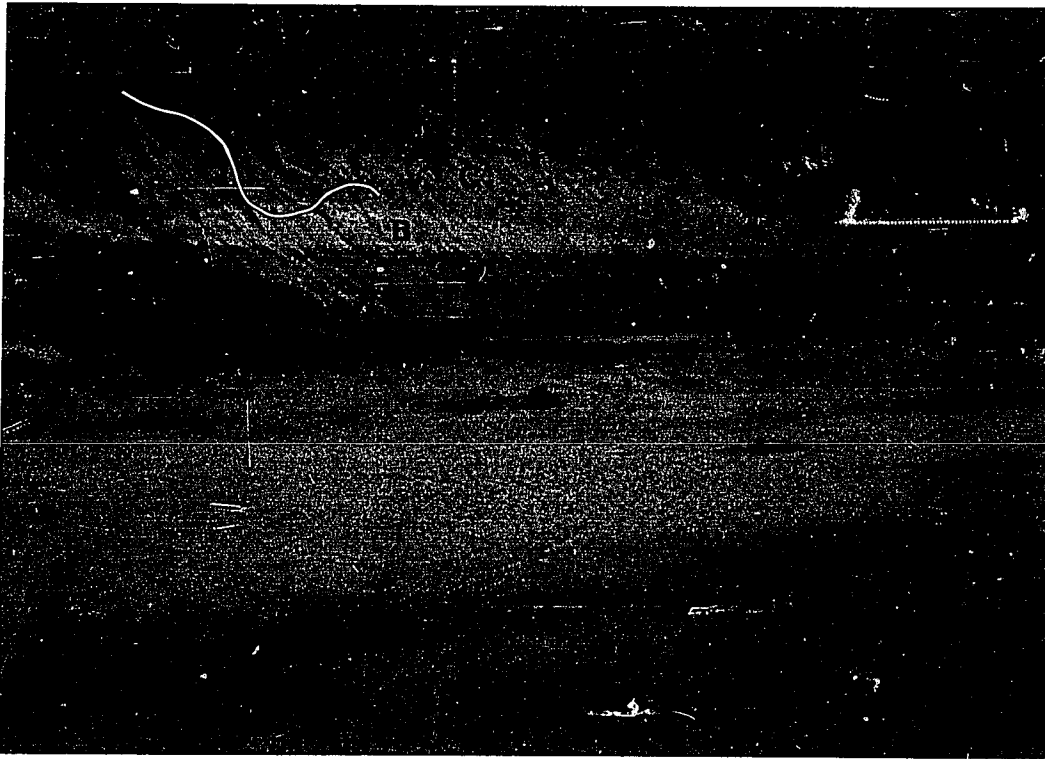


Figure 23. Wind-carved exposure at northeast margin of E-32, revealing: late Wisconsin pluvial and interpluvial sediments (A), lenticular Meinzer Dune (B), Willard Playa/Dune Complex parabolic-dune sediments (C).

precipitation and the associated rise of groundwater levels that probably produced standing water in the basins. The subsequent rise in pore water pressure and decreased effective stress led to instability and the resulting earthflow event.

The modern phase is dominated by several active processes, the most pronounced of which is deflation. Since the time of flowage, deflation has removed over 8,200,000 m<sup>3</sup> of earthflow sediment from the basin floors. Modern arroyo cutting and slumping occur in response to high-intensity, sporadic precipitation, and are caused by low infiltration and high surface runoff. Lateral expansion, that truncates earthflow scars and modifies deflation basin morphology, results from wave erosion and eolian activity. Wave erosion occurs following periods of high-intensity precipitation when there is standing water in the deflation basins. Eolian activity is responsible for large active areas concentrated along west-southwest facing slopes. These processes are presently elongating deflation basin geometry along a northeast trend.

### REGIONAL IMPLICATION

This section presents geomorphic evidence for a more mesic late Holocene from the Lake Willard Playa/Dune Complex. The late Holocene, as noted in figure 4, is defined as the time from 3,000 yr B.P. to the present. The late-middle Holocene, as referred to in this section, ranges from approximately 5,000 to 3,000 yr B.P. Similarities between the Estancia Valley late Holocene record and other areas in the southwest suggest that paleoclimatic correlations can be made.

There are several factors that must be considered when attempting to make regional correlations. Foremost is that conditions within adjacent valleys

may respond differently to external variables. Waters (1986), documents the Holocene history of two adjacent valleys in southeast Arizona where the differing alluvial records were caused by independent intrinsic geomorphic thresholds peculiar to each basin. In the Estancia Valley watershed, for example, recharge on the west side of the valley is 5 times higher than on the east due to runoff from the Manzano Mountains (Smith and Anderson, 1982). This suggests that climatic oscillations in the Manzano Mountains will affect groundwater levels in the central valley.

#### **LATE-MIDDLE HOLOCENE**

Although it is generally agreed that the middle Holocene was a time of increased temperatures, there are conflicting reports on the amount of effective moisture. Martin (1963), Mehringer and others (1967) Van Devander and Wiseman (1977), and Spaulding (1983), document environments in the Sonoran, Mohave, and Chihuahuan deserts that indicate the middle Holocene was a time of increased effective moisture. Antevs (1955), Gile (1979), Gaylord (1982), Aikens (1983), Dean and others (1984), Meltzer and Collins (1987), Winkler and others (1986), and Holiday (1985; 1989), document environments indicating that the middle Holocene in the Great Plains, midwest, and southwest was warmer and had less effective moisture (Fig. 24).

Near the Estancia Valley, in the Southern High Plains, Holiday (1989), documents a dry, warm middle Holocene based on geomorphic evidence that is supported by C<sup>14</sup> dates. These sites reflect pulses of eolian activity culminating between 6,000 and 4,500 yr B.P.

In the Estancia Valley, termination of the Meinzer subpluvial and the beginning of basin deflation documents a middle to late-middle Holocene marked by increased temperatures, continued high winds, and decreased effective

ka			Southern Deserts (Spaulding, 1983)	Southern Deserts (Aikens, 1983)	Southern High Plains (Holiday, 1989)	Mohave Desert (La Marche, 1974)	Estancia
0	L A T E	L a t e		↕ Dry		⊕ Warm * Cool * Warm	↕ Warm and Dry * ?
1				↕ Wet		* Cool * Warm	* ? * ?
2	H O L O C E N E	M i d d l e		⊕ Wet		⊕ Cool * Warm	* Very Wet * ?
3			E a r l y				* Cool * Warm
	M I D D L E	L a t e		Warm and Wet	Warm and Dry	Warm and Dry	* Warm and Dry * ?

Figure 24. Chart comparing climatic similarities and differences between various regions of the southwest for the late-middle to late Holocene.

moisture. Although the duration of the thermal maximum differs from region to region, a charcoal-rich soil horizon dated at 4,660 yr B.P. in the lower sediments of the Willard Playa/Dune Complex suggests the thermal maximum in the Estancia Valley commenced at approximately 5,000 yr B.P. This places the thermal maximum (i.e. Altithermal) in the Estancia Valley later than in other areas. Furthermore, this record indicates that the Estancia Valley responded similarly to the Southern High Plains during the middle to late-middle Holocene. In contrast, it responded differently, or was not under the same climatic influence as were the Sonoran and Mohave Deserts.

Although it is situated in the Basin and Range Province, as are the western deserts, the topography and the regional setting of the Estancia Valley are more similar to the Southern High Plains and correlation of the valley to the Southern High Plains during the Holocene is probably more realistic.

## **LATE HOLOCENE**

Spaulding (1983), notes that records of climatic fluctuation in the southwest are ubiquitous during the late Holocene, but that these records usually document changes that are less pronounced in comparison to the early and middle Holocene.

Although our understanding of late Holocene fluctuations is incomplete, late-Holocene time was marked by increased moisture and decreased temperatures. In the Mohave Desert, the onset of the late Holocene was marked by a decrease in summer temperatures (La Marche, 1973), and an increase in effective moisture relative to the middle Holocene and the present (Spaulding, 1983). Glasner (1981), and Winkler and others (1986), document colder and wetter conditions in the late Holocene of the midwest, and Burke and Birkland (1983), document regrowth of alpine glaciers during the intermediate and late

Neoglacial phases ( <3,000 yr B.P) (Fig. 24).

Interpreting from the archeologic record, Aikens (1983), provides detailed paleoecologic evidence for increased effective moisture during the late Holocene of the southwest. The record suggests that many of the cultural sites were abandoned between 5 to 7,000 yr B.P, due to dry conditions during the middle Holocene. An expansion of the local cultural communities is evidenced during the late Holocene when effective moisture again increased. According to Aikens (1983), archaeological data for the last 2,000 years is even more abundant. Hydrologic and pollen evidence indicates a peak in the effective moisture level from 1,350 to 1,250 yr B.P. and from 1,000 to 800 yr B.P. In contrast, a shift in the human population centers and the appearance of water-control devices marks the return of dryer conditions at approximately 500 yr B.P., which is also the time of pueblo abandonment (Aikens, 1983).

In the Mohave Desert, La Marche (1974), made paleoclimatic interpretations based on dendrochronology. His reconstructions were based on the idea that trees respond to the general regional climate, therefore, assessments can be made for areas outside the tree-ring network (Brubaker and Cook, 1983). In a 5,405 year-long chronology, La Marche (1974), interprets warm periods from 5,500 to 3,300 yr B.P., 2,000 to 1,950 yr B.P., 800 to 600 yr B.P., and 100 yr B.P. to the present. He also indicates cooler periods were present from 3,300 to 2,000 yr B.P., 1,700 to 800 yr B.P., and 600 to 100 yr B.P. The warm period from 5,500 to 3,300 yr B.P. is believed to correlate with initiation of the Willard Playa/Dune Complex and the onset of the thermal maximum in the Estancia Valley.

In the Estancia Valley, the basin-fill and earthflow phase document a late Holocene increase in effective moisture, and a probable decrease in temperature. These observations are consistent with those described in the Mohave Desert as well as those in the Great Plains and midwest.

Aikens (1983), who documents increased effective moisture from 1,350 to 1,250 yr B.P. and from 1,000 to 800 yr B.P. makes the most comprehensive assessment of late Holocene mesic fluctuations. It should be noted that his first interval falls completely within the cooler period (1,700 to 800 yr B.P.) bracketed by La Marche (1974). The second interval also has a 200 year overlap. These periods of increased moisture, especially the former, may have triggered the earthflow event in the Estancia Valley. Because absolute dates are lacking, constraints on the timing of the earthflow event and assigning it to a specific time, however, is speculative.

In the latest Holocene of the Mohave Desert, Spaulding (1983), documents a shift to more xerophytic plant assemblage at about 300 yr B.P. However, he notes that this may be due to cattle grazing in the late 19th and 20th century. Based on tree-ring studies, La Marche (1974) notes two warm periods; 800 to 600 yr B.P. and 100 yr B.P. to the present. Aikens (1983) in his paleoclimatic reconstruction, designates a hiatus in decreased effective moisture at 500 yr B.P. These dates suggest that more xeric conditions returned to the southwest at approximately 800 to 300 yr B.P.

In the Estancia Valley, a shift to xeric conditions of the latest Holocene is supported by the modern phase of the Willard Playa/Dune Complex. Termination of the earthflow phase, which indicates a decrease and shift in precipitation, as well as probable increased wind activity and temperature, also supports this shift. This phase probably occurred at approximately 500 yr B.P. The present topography, however, indicates that water, from high-intensity precipitation events, still plays a major role in the erosional processes of the valley.

## SUMMARY

The history of the Willard Playa Complex documents several climatic fluctuations from the late-middle Holocene to the present. These fluctuations can be correlated regionally, but due to a lack of absolute dates, many confining ages are not known and specific assignments remain questionable. Formation of the Willard Playa/Dune Complex commenced at approximately 5,000 yr B.P. with more xeric conditions following the Meinzer subpluvial. These xeric conditions are believed to be correlative with the late-middle Holocene.

The ensuing basin-fill and earthflow phase, beginning at the onset of the late Holocene, confirms a documented increase in effective moisture relative to the middle Holocene and the present. The earthflow phase thus represents culmination of more mesic conditions within the late Holocene and documents increased precipitation in the Estancia Valley. Based on similar geomorphic preservation, the relative ages of the earthflow scars are probably time synchronous, therefore, the climatic event that induced the flows represents a distinct short term event. Furthermore, the distinct morphology of the scars indicate that the climatic event was quite recent. It is conceivable, for instance, that the flows may be only centuries old. The exact age is speculative, nevertheless the earthflows of the Willard Playa/Dune Complex are time stratigraphic markers for a more mesic interval within the late Holocene of the Estancia Valley.

Increased eolian activity and decreased precipitation in the modern phase mark a return to more xeric conditions throughout the southwest. This phase represents a time of decreased annual rainfall, and a shift toward low frequency, high intensity convectional type precipitation.

## REFERENCES

- Aikens, C. M., 1983, Environmental archaeology of the western United States, in Wright, H. E., Jr., ed., Late-Quaternary environments of the United States: The Holocene: Minneapolis, Minnesota, University of Minnesota Press, p. 293-251.
- Allen, J. R. L., 1985, Physical sedimentology: London, Allen and Unwin, 272 p.
- 1982, Sedimentary structures, their character and physical basis: v. II, Amsterdam, Elsevier, 663 p.
- Antevs, E., 1954, Climate of New Mexico during the last glacio-pluvial: Journal of Geology, v. 62, p. 182-191.
- 1955, Geologic-climatic dating in the west: American Antiquity, v. 20, p. 317-335.
- Bachhuber, F. W., 1971, Paleolimnology of Lake Estancia and the Quaternary history of the Estancia valley [Ph.D thesis]: Albuquerque, New Mexico, University of New Mexico, 238 p.
- 1982, Quaternary history of the Estancia Valley, central New Mexico, in Grambling, J. A., and Wells, S. G., eds., Albuquerque Country II: New Mexico Geological Society, 33rd Field Conference, Guidebook, p. 343-346.
- 1987, An early mid-Wisconsin climatic record from the Estancia Valley, central New Mexico: Geological Society of America Abstracts with Programs, v. 19, p. 577.
- 1988, Paleontologic analysis of an early through middle Wisconsin section from the Estancia Valley, central New Mexico: Geological Society of America Abstracts with Programs, v. 20, p. 206.
- Bachhuber, F. W., and McClellan, W. A., 1977, Paleoecology of marine Foraminifera in the pluvial Estancia Valley, central New Mexico: Quaternary Research, v. 7, p. 254-267.
- Blackwelder, E., 1912, The Gros Ventre slide, an active earth-flow: Geological Society of America Bulletin, v. 23, p. 487-492.
- Bourlier, B. G., Neher, R. E., Crezee, D. B., Bowman, K. J., and Meister, D.W., 1970, Soil survey of Torrance area, New Mexico: United States Department of Agriculture and New Mexico Agricultural Experiment Station, 149 p.
- Bowler, J. M., 1976, Aridity in Australia; Age, origins and expressions in aeolian landforms and sediments: Earth Science Review, v. 12, p. 279-310.

- 1986, Spatial variability and hydrologic evolution of Australian lake basins: Analogue for Pleistocene change and evaporite formation: *Paleogeography, Paleoclimatology, and Paleoecology*, v. 54, p. 21-41.
- Bowler, J. M., and Teller, J. T., 1986, Quaternary evaporites and hydrologic changes, Lake Tyrell, north-west Victoria: *Australian Journal of Earth Sciences*, v. 33, p. 43-63.
- Bowler, J. M., and Wasson, R. J., 1986, Semi-arid and arid zones of southeastern Australia and Lake Frome and Strzelecki Desert: 12th International Sedimentological Congress, p. 10-36.
- Brakenridge, G. R., 1978, Evidence for a cold, dry full-glacial climate in the American southwest: *Quaternary Research*, v. 9, p. 22-40.
- Brodzikowski, K., and Haluszczak, A., 1987, Flame structures and associated deformations in Quaternary glaciodeltaic deposits: examples from central Poland, *in* Jones, M. E., and Preston, R. M. F., eds., *Deformation of sediments and sedimentary rocks: Geological Society Special Publication 29*, p. 279-286.
- Brubaker, L. B., and Cook, E. R., 1983, Tree-ring studies of Holocene environments, *in* Wright, H. E., Jr., ed., *Late-Quaternary environments of the United States: The Holocene: Minneapolis, Minnesota, University of Minnesota Press*, p. 222-235.
- Burke, R. M., and Birkeland, P. W., 1983, Holocene glaciation in the mountain ranges of the western United States, *in* Wright, H. E., Jr., ed., *Late-Quaternary Environments of the United States: The Holocene: Minneapolis, Minnesota, University of Minnesota Press*, p. 3-11.
- Chowdury, R. N., 1978, *Slope analysis: New York, Elsevier*, 423 p.
- Coates, D. R., 1977, Landslide perspectives, *in* Coates, D. R., ed., *Landslides, Reviews in engineering geology*, v. III: *Geological Society of America*, p. 3-28.
- Dean, W. E., Bradbury, J. P., Anderson, R. Y., and Barnosky, C. W., 1984, The variability of Holocene climatic change; evidence from varved lake sediments: *Science*, v. 226, p. 1191-1194.
- Deer, W. A., Howie, R. A., and Zussman, J., 1966, *An introduction to the rock forming minerals: England, Longman Group*, 528 p.
- Eckel, E. B., ed., 1958, *Landslides and engineering practice: National Research Council, Highway Research Board Special Report 29*, 232 p.
- Eden, W. K., and Mitchell, R. J., 1973, Landslides in sensitive marine clay in eastern Canada: *Highway Research Record 463*, p.18-63.
- Freeze, R. A., and Cherry, J. A. 1979, *Groundwater: Englewood Cliffs, New Jersey, Prentice-Hall*, 604 p.

- Gabler, R. E., Brazier, S., Sager, R. J., and Wise, D. L., 1982, *Essentials of physical geography*: Philadelphia, Saunders, 568 p.
- Galloway, R. W., 1970, The full-glacial climate in the southwestern United States: *Annals of the Association of American Geographers*, v. 60, p. 245-256.
- Gaylord, D. R., 1982, Geologic history of the Ferris Dune Fields south-central Wyoming, in Marrs, R. W., and Kolm, K. E., eds., *Interpretation of windflow characteristic from eolian landforms*: Geological Society of America Special Paper 192, p. 65-82.
- Gile, L. H., 1979, Holocene soils in eolian sediments of Bailey County, Texas: *Soil Science Society of America Journal*, v. 43, p. 994-1003.
- Glasner, P. H., Wheeler, G. A., Gorham, E., and Wright, H. E., Jr., 1981, The patterned mires of Red Lake peatland, northern Minnesota, vegetation, water chemistry, and landforms: *Journal of Ecology*, v. 69, p. 575-599.
- Harbour, J., 1958, *Microstratigraphic and sedimentologic studies of an early man site near Lucy, New Mexico* [M.S. thesis]: Albuquerque, New Mexico, University of New Mexico, 111 p.
- Holiday, V. T., 1985, *Archaeological geology of the Lubbock Lake site, Southern High Plains of Texas*: Geological Society of America Bulletin, v. 96, p. 1483-1492.
- \_\_\_\_\_, 1989, Middle Holocene drought on the Southern High Plains: *Quaternary Research*, v. 31 p. 74-82.
- Howe, E., 1909, *Landslides in the San Juan Mountains, Colorado*: United States Geological Survey Professional Paper 67, 58 p.
- Huang, Y. H., 1983, *Stability analysis of earth slopes*: New York, Van Nostrand, 305 p.
- Keefer, D. K., and Johnson, A. M., 1983, *Earth flows: Morphology, mobilization, and movement*: U.S. Geological Survey Professional Paper 1264, 56 p.
- Kelling, G., and Walton, E. K., 1957, Load-cast structures: their relationship to upper surface structures and their mode of formation: *Geological Magazine*, v. 94, v. 481-90.
- Kelly, V. C., 1972, *Geology of the Fort Summner Sheet, New Mexico*: New Mexico Bureau of Mines and Mineral Resources, Bulletin 98, 51 p.
- La Marche, V. C., 1973, Holocene climatic variations inferred from treeline fluctuations in the White Mountains, California: *Quaternary Research*, v. 3, p. 632-660.
- \_\_\_\_\_, 1974, Paleoclimatic inferences from long tree-ring records: *Science*, v. 183, p. 1043-48.

- Leopold, L. B., 1951, The Pleistocene climate in New Mexico: *American Journal of Science*, v. 249, p. 152-168.
- Lyons, T. R., 1969, A study of the Paleo-Indian and desert culture complexes of the Estancia Valley area, New Mexico [Ph.D thesis]: Albuquerque, New Mexico, University of New Mexico, 335 p.
- Machette, M. N., 1982, Quaternary and Pliocene faults in the La Jencia and southern part of the Albuquerque and Belen basins, New Mexico: evidence of fault history from fault-scarp morphology and Quaternary geology, *in* Grambling, J. A., and Wells, S. G., eds., *Albuquerque Country II: New Mexico Geological Society, 33rd Field Conference, Guidebook*, p. 161-170.
- Martin, P. S., 1963, The last 10,000 years--A fossil pollen record of the American Southwest: Tucson, University of Arizona Press, 87 p.
- Mathewson, C. C., 1981, *Engineering Geology*: Columbus, Ohio, Charles E. Merrill, 410 p.
- Mehringer, P. J., Jr., Martin, P. S., and Haynes, C. V., Jr., 1967, Murray Springs, a mid-postglacial pollen record from southern Arizona: *American Journal of Science*, v. 265, p. 786-797.
- Meinzer, O. E., 1911, Geology and groundwater resources of the Estancia Valley, New Mexico; with notes on groundwater conditions in adjacent part of central New Mexico: U.S. Geological Survey Water-Supply Paper 275, 89 p.
- Meltzer, D. J., and Collins, M. B., 1987, Prehistoric water wells on the Southern High Plains; Clues to Altithermal climate: *Journal Field Archeology*, v. 14, p. 9-27.
- Mills, P. C., 1982, Genesis and diagnostic value of soft sediment deformation structures--a review: *Sedimentary Geology*, v. 35, p. 83-104.
- Mitchell, R. J., 1976, Earthflow terrain evaluation in Ontario: Kingston, Ontario, Queens University, Department of Civil Engineering Final Report, Project Q-53, 23 p.
- Mitchell, R. J., and Markel, 1974, Flowsliding in sensitive soils: *Canadian Geotechnical Journal*, v. 11, p. 11-31.
- Mollard, J. D., 1977, Regional landslide types in Canada, *in* Coates, D. R., ed., *Landslides, Reviews in engineering geology III: Geological Society of America*, p. 29-56.
- Morgenstern, N. R., 1971, Influence of groundwater on stability, *in* Brawner, C. O., and Milligan, V., eds., *Stability in open pit mining: American Institute of Mining, Metallurgical, and Petroleum Engineers*, p. 65-83.

- Morgenstern, N. R., and Sangrey, D. A., 1978, Methods of stability analysis, in Schuster, R. J., and Krietzek, R. L., eds., Landslides--analysis and control: National Academy of Sciences, Transportation Research Board Special Report 176, p. 155-169.
- Northrop, S. A., 1982, Earthquakes of the Albuquerque country, in Grambling J. A., and Wells, S. G., eds., Albuquerque Country II: New Mexico Geological Society, 33rd Field Conference, Guidebook, p. 171-178.
- Osterkamp, W.R., and Wood, W. W., 1987, Playa-lake basins on the Southern High Plains of Texas and New Mexico: Part I. Hydrologic, geomorphic, and geologic evidence for their development: Geological Society of America Bulletin, v. 99, p. 215-223.
- Owen, G., 1987, Deformation processes in unconsolidated sands, in Jones, M. E., and Preston, R. M. F., eds., Deformation of sediments and sedimentary rocks: Geological Society Special Publication 29, p. 11-24.
- Price, W. A., 1963, Physiochemical and environmental factors in clay dune genesis: Journal of Sedimentary Petrology, v. 33, p. 766-778.
- Roth, E. S., 1960, The silt-clay dunes at Clark Dry Lake, California: Compass, v. 38, p. 18-27.
- Schuster, R. J., and Krietzek, R. L., eds., 1978, Landslides- analysis and control: National Academy of Sciences, Transportation Research Board Special Report 176, 234 p.
- Sharp, C. F. S., 1939, Landslides and related phenomena: New York, Cooper Square Publishers, 137 p.
- Smith, R. E., 1957, Geology and groundwater resources of Torrance County, New Mexico: New Mexico Bureau of Mines and Mineral Resources Groundwater Report 5, 186 p.
- Smith, L. N., and Anderson, R. Y., 1982, Pleistocene-Holocene climate of the Estancia Basin, central New Mexico, in Grambling, J. A., and Wells, S. G., eds., Albuquerque Country II: New Mexico Geological Society, 33rd Field Conference, Guidebook, p. 347-350.
- Spaulding, W. G., 1983, Vegetation and climates of the last 45,000 years in the vicinity of the Nevada Test Site, south-central Nevada: United States Geological Survey Open-File Report 83-535, 199 p.
- Tavenas, F., Chagnon, J. Y., and LaRochelle, P., 1971, The Saint Jean-Vianney landslide; observations and eyewitness accounts: Canadian Geotechnical Journal, v. 8, p. 315-335.
- Titus, F. B., 1969, Late Tertiary and Quaternary hydrogeology of the Estancia basin, central New Mexico [Ph.D thesis] Albuquerque, New Mexico, University of New Mexico, 179 p.

- United States Department of Agriculture, Soil Conservation Service, 1960, Soil classification; a comprehensive system, 7th approximation, 265 p.
- Van Devander, T. R., and Wiseman, F. M., 1977, A preliminary chronology of bioenvironmental changes during the paleoindian period in the monsoonal southwest, *in* Johnson, E., ed., *Paleoindian lifeways: Lubbock West Texas Museum Association, The Museum Journal*, v. 17, p. 13-27.
- Varnes, D. J., 1978, Slope movement type and processes, *in* Schuster, R. J., and Kriezek, R. L., eds., *Landslides--analysis and control: National Academy of Sciences, Transportation Research Board Special Report 176*, p. 12-33.
- Velde, B., and Meunier, A., 1987, Petrologic phase equilibria in natural clay systems, *in* Newman, A. C. D., ed., *Chemistry of clays and clay minerals: Mineralogical Society, monograph 6*, p. 423-458.
- Wasson, R. J., 1983, Dune sediment types, sand colour, and sediment provenance and hydrology in the Strzelecki-Simpson dunefield, Australia, *in* Brookfield, M. E., and Albrandt, T. S., eds., *Eolian sediments and processes: Amsterdam, Elsevier*, p. 165-195.
- Waters, M. R., 1986, *Geoarchaeology of Whitewater Draw, Arizona: Anthropological Papers of the University of Arizona*, no. 45, 181 p.
- Weide, D. L., 1975, *Post-glacial geomorphology and environments of the Warner valley and Hart Mountain area, Oregon [Ph.D thesis]: Los Angeles, California, University of California*, 293 p.
- Winkler, M. G., Swain, A. M., and Kutzbach, J. E., 1986, Middle Holocene dry period in the northern midwestern United States: *Quaternary Research*, v. 25, p. 235-250.
- Woodward, L. E., 1982, Tectonic framework of Albuquerque Country, *in* Grambling, J. A., and Wells, S. G., eds., *Albuquerque Country II: New Mexico Geological Society, 33rd Field Conference, Guidebook*, p. 141-145.
- Zaruba, Q., and Mencl, V., 1969, *Landslides and their control: Amsterdam, Elsevier*, 205 p.

## APPENDIX 1

## Major Oxide Geochemical Analysis

%	Sample E-28-DC-1	E-32-MD-2
SiO <sub>2</sub>	24.07	8.86
Al <sub>2</sub> O <sub>3</sub>	5.61	2.14
Fe <sub>2</sub> O <sub>3</sub>	2.41	1.10
MgO	2.82	1.37
CaO	22.78	29.05
Na <sub>2</sub> O	0.76	0.62
K <sub>2</sub> O	2.32	1.41
TiO <sub>2</sub>	0.23	0.09
P <sub>2</sub> O <sub>5</sub>	0.28	0.22
MnO	0.04	0.02
BaO	0.07	0.03
LOI	21.69	22.03
Total	83.09	66.94
Co <sub>2</sub> (inorg)	9.48	4.61
SO <sub>4</sub>	19.70	41.49
S	6.39	13.20

## APPENDIX 2

## Results of Sieve Analysis

Outcrop						
Dry Sieve	1	2	3	4	5	Pan
E-28-YH	12.0	31.3	37.6	10.0	4.6	4.3
E-28-DC-2	7.4	24.0	43.5	15.8	5.5	4.2
E-28-F2-FR-3	9.5	34.3	38.6	11.6	3.3	3.3
Wet Sieve						
E-28-YH	4.0	18.1	28.5	14.1	6.4	28.9
E-28-DC-2	1.4	11.4	2.3	14.4	7.0	43.5
E-28-F2-2	6.9	16.0	19.1	9.3	5.3	43.4
E-28-F2-FR-3	2.9	17.6	18.3	9.3	4.8	47.1
E-28-F2-FR-4	3.3	17.2	18.6	10.0	3.9	46.8
E-28-F2-FR-5	2.9	26.3	24.6	10.8	5.8	29.6
E-28-F5-FR-1	24.1	16.6	14.7	8.8	4.9	30.8
E-13-F4-1	2.5	12.6	35.7	13.5	3.8	31.9
E-13-F4-2	3.1	13.1	35.5	12.4	4.3	31.3
Augered Samples (m)						
E-28-F2-3	1	2	3	4	5	pan
0	2.0	6.8	13.5	10.0	6.1	61.5
0.75	1.3	9.0	13.6	14.3	7.3	54.0
1.5	1.3	8.5	17.0	14.7	7.5	51.0
2.25	3.6	10.0	20.0	18.0	10.0	38.0
2.75	1.3	10.6	20.3	12.7	6.7	48.3
3.5	1.6	8.6	16.6	10.3	5.0	57.6
4.25	5.4	11.1	16.9	8.7	5.4	52.4
5.0	2.0	8.0	18.0	11.3	5.3	55.3
5.75	1.5	10.3	16.6	9.1	4.5	57.9
6.0	2.5	7.0	17.0	11.3	6.3	56.0
6.5	2.6	10.6	15.2	8.1	4.5	59.0
7.0	1.9	10.4	16.8	9.5	4.4	57.0
7.75	1.4	7.0	14.6	9.6	5.3	62.1
8.5	3.4	4.5	11.2	9.3	4.2	67.4
9.0	3.9	6.5	10.4	10.4	5.0	63.9
E-28-F2-2	1	2	3	4	5	pan
0	-	-	-	-	-	-
0.75	2.5	3.9	9.2	8.9	5.7	69.9
1.5	2.2	7.5	17.7	14.5	7.5	51.0
2.25	1.8	7.3	16.4	16.8	10.9	46.8
3.0	2.8	19.0	23.1	12.2	5.7	37.6
3.75	2.1	13.1	18.4	19.8	4.9	36.5
4.5	3.3	12.9	17.5	12.5	4.6	49.2
5.25	2.8	5.8	12.3	6.0	3.5	69.7
6.0	3.5	5.5	9.1	8.0	3.8	70.0
6.75	13.0	14.0	20.8	11.3	4.0	37.0
7.25	46.2	9.0	9.0	8.6	3.6	23.7
E-28-F2-1						
0	7.8	7.8	11.0	10.0	8.0	55.5
0.75	3.7	25.7	23.3	12.2	6.1	29.0
1.5	5.2	11.4	16.1	7.9	4.4	54.9
2.10	23.4	11.2	12.2	7.3	4.3	42.2

NOTE: Large +1 phi values at the bottom of holes is due, in part, to lacustrine clay aggregates. This was accounted and adjusted for when generating sand versus clay/silt ratios.

**PLATE 1**

**SURFICIAL GEOLOGIC MAP OF THE WILLARD PLAYA/DUNE  
COMPLEX, ESTANCIA VALLEY, NEW MEXICO**

(in pocket)

**PLEASE NOTE:**

Oversize maps and charts are filmed in sections in the following manner:

**LEFT TO RIGHT, TOP TO BOTTOM, WITH SMALL OVERLAPS**

The following map or chart has been refilmed in its entirety at the end of this dissertation (not available on microfiche). A xerographic reproduction has been provided for paper copies and is inserted into the inside of the back cover.

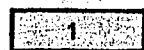
Standard 35mm slides or 17" x 23" black and white photographic prints are available for an additional charge.

**U·M·I**

## EXPLANATION

Expanding on a 1:31,000 surficial geologic map of the Estancia Valley (Bachhuber, 1971), this map focuses on the deflation basins, dunes, and earthflow scars of the Willard Playa/Dune Complex.

### Earthflows:



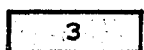
#### SLIGHTLY MODIFIED EARTHFLOW SCARS (TYPE 1)

Scars are easily discernible and original morphology is well preserved; scars exhibit long distinct sidewalls, sharp headwall crowns, and flat bottomed floors with a continuous slope. The scars are not extensively cut by arroyos or modified by eolian activity. These scars are the most recent.



#### MODIFIED EARTHFLOW SCARS (TYPE 2)

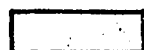
Discernible but original morphology modified by eolian activity and arroy cutting. Headwalls often appear as blowouts at the dune crest. Sidewalls are preserved but are modified and less distinct than type 1. Floors are more scalloped and dissected by arroyos.



#### GREATLY MODIFIED EARTHFLOW SCARS (TYPE 3)

Not distinguishable from deflation scours. Original morphology highly obscured and modified by eolian activity. Head and sidewalls are not distinct and original dune slope is rarely preserved between adjacent flows. Floors are scalloped and dissected by arroyos.

### Surficial and Geomorphic Units:



#### WILLARD DUNES

Coarse sand to fine silt-sized gypsum with 60% clay pellets; moderate sorting. Indistinctive small and large scale cross-bedding; gypsiferous units common. Sediments are derived from pre-existing Meinzer Dunes and underlying lacustrine sediments. Dune thickness attains 30 m; generally stabilized but with locally active areas.



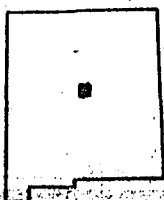
#### PLAYA-FLOORED DEFLATION BASINS

Silty-sand to clay, distinct laminae of organic, inorganic, and gypsiferous units. Generally, 0-1 m thick. Commonly encrusted with salt and/or gypsum. Forms floors of active deflation basins.

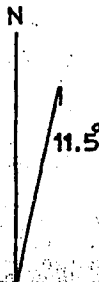


#### DEFLATION BASIN FLOORS

Partially vegetated and stable with minor topography. Forms floors of inactive deflation basins.



New Mexico



SCALE 1:24 000

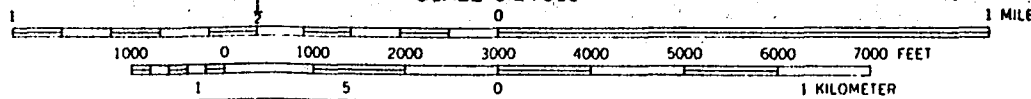




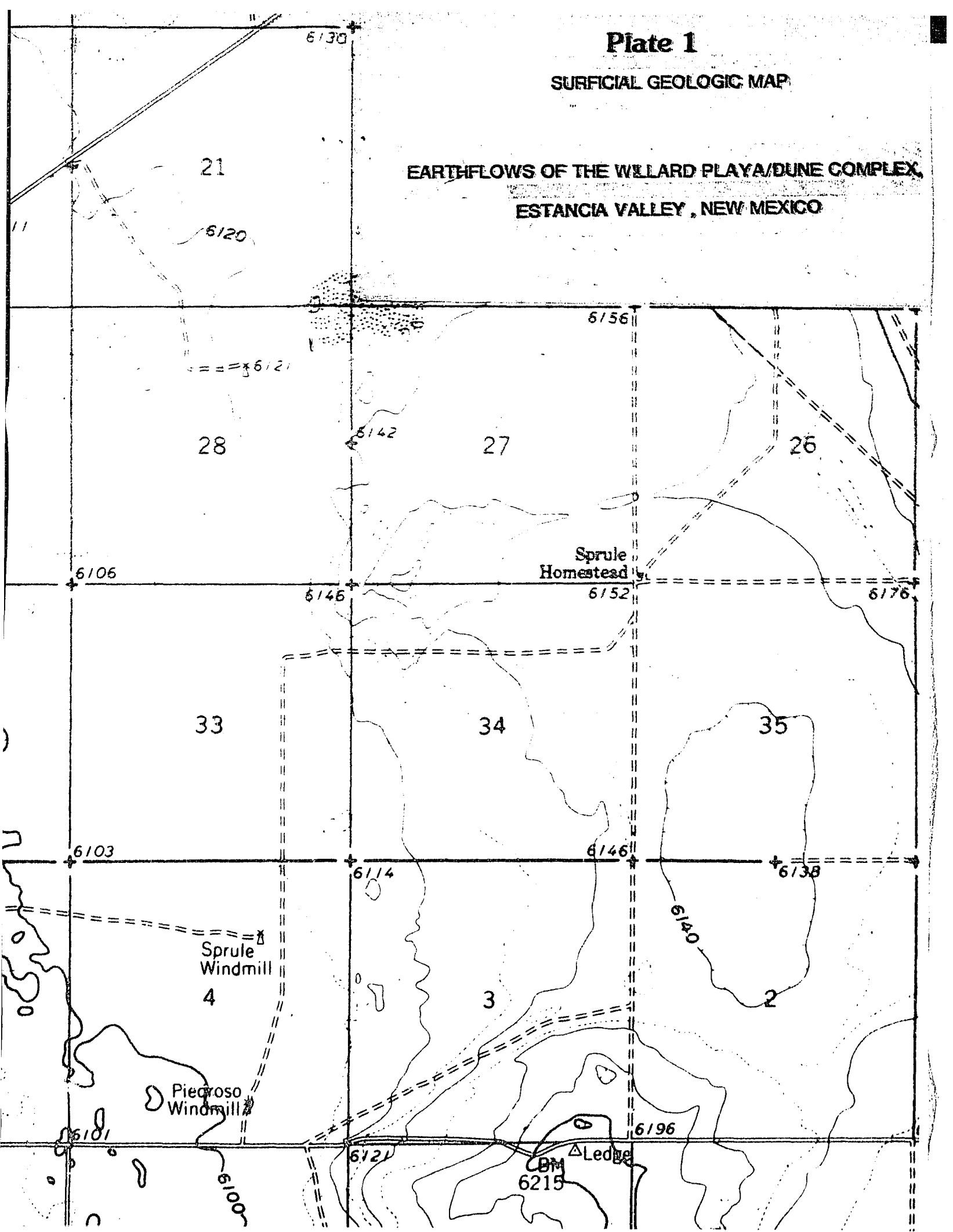




# Plate 1

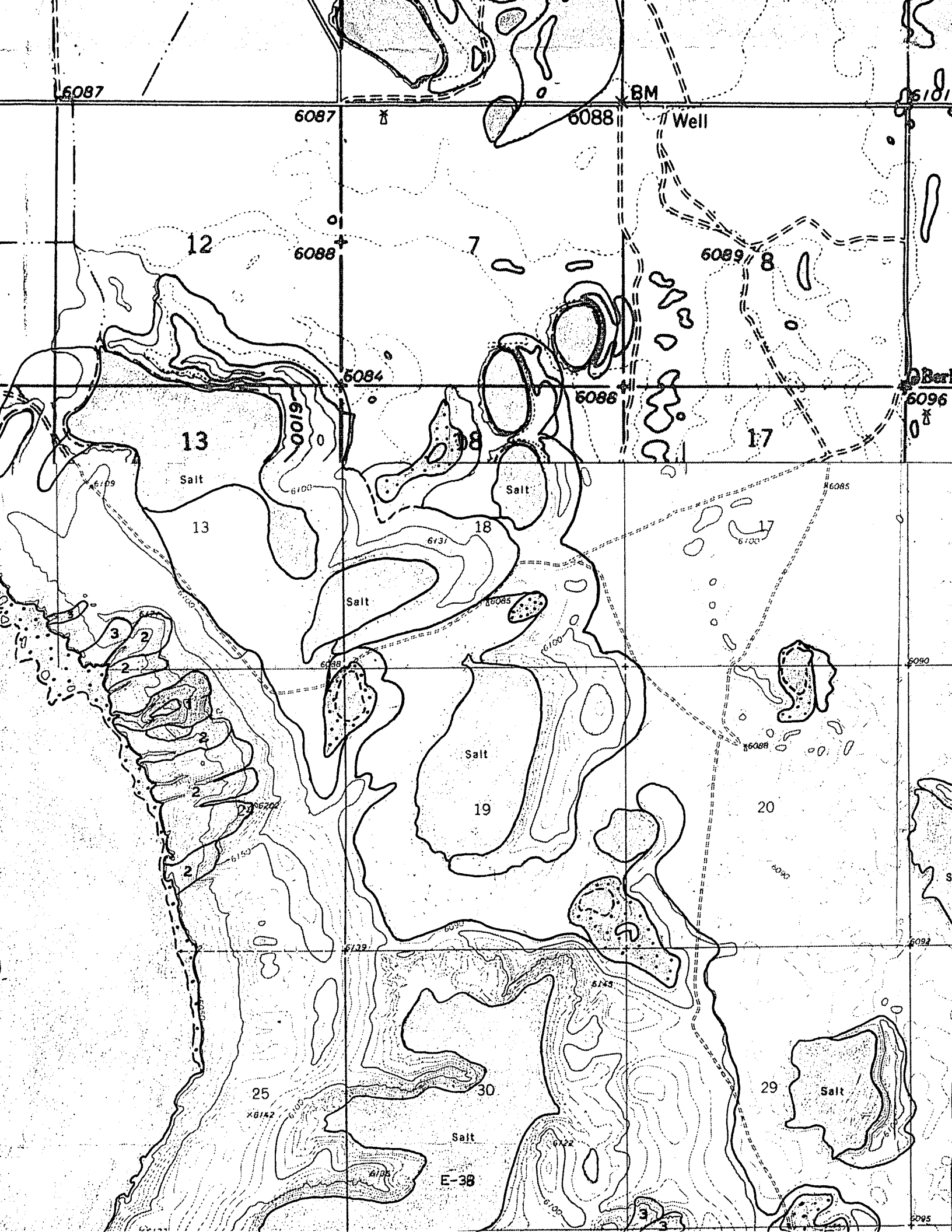
## SURFICIAL GEOLOGIC MAP

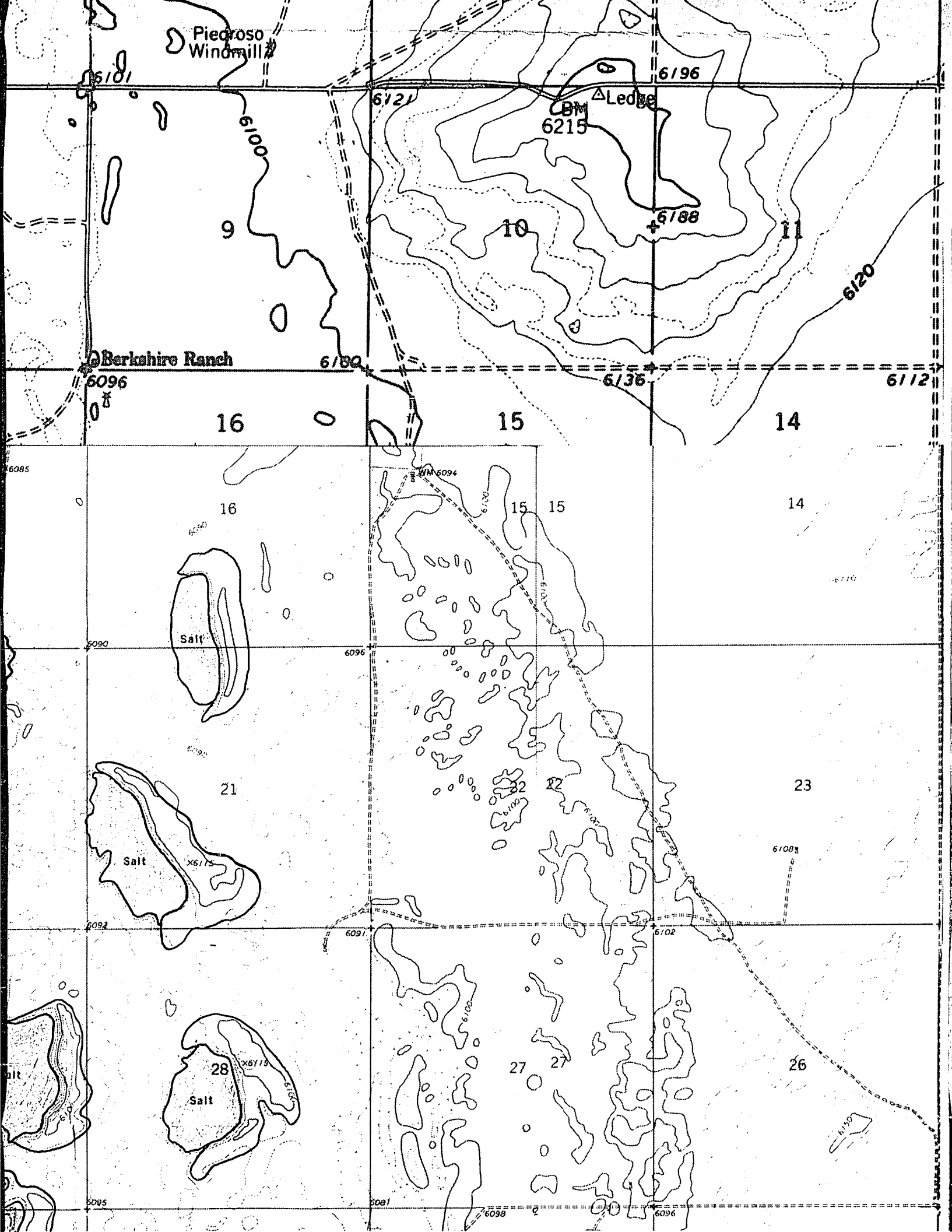
### EARTHFLOWS OF THE WILLARD PLAYA/DUNE COMPLEX, ESTANCIA VALLEY, NEW MEXICO

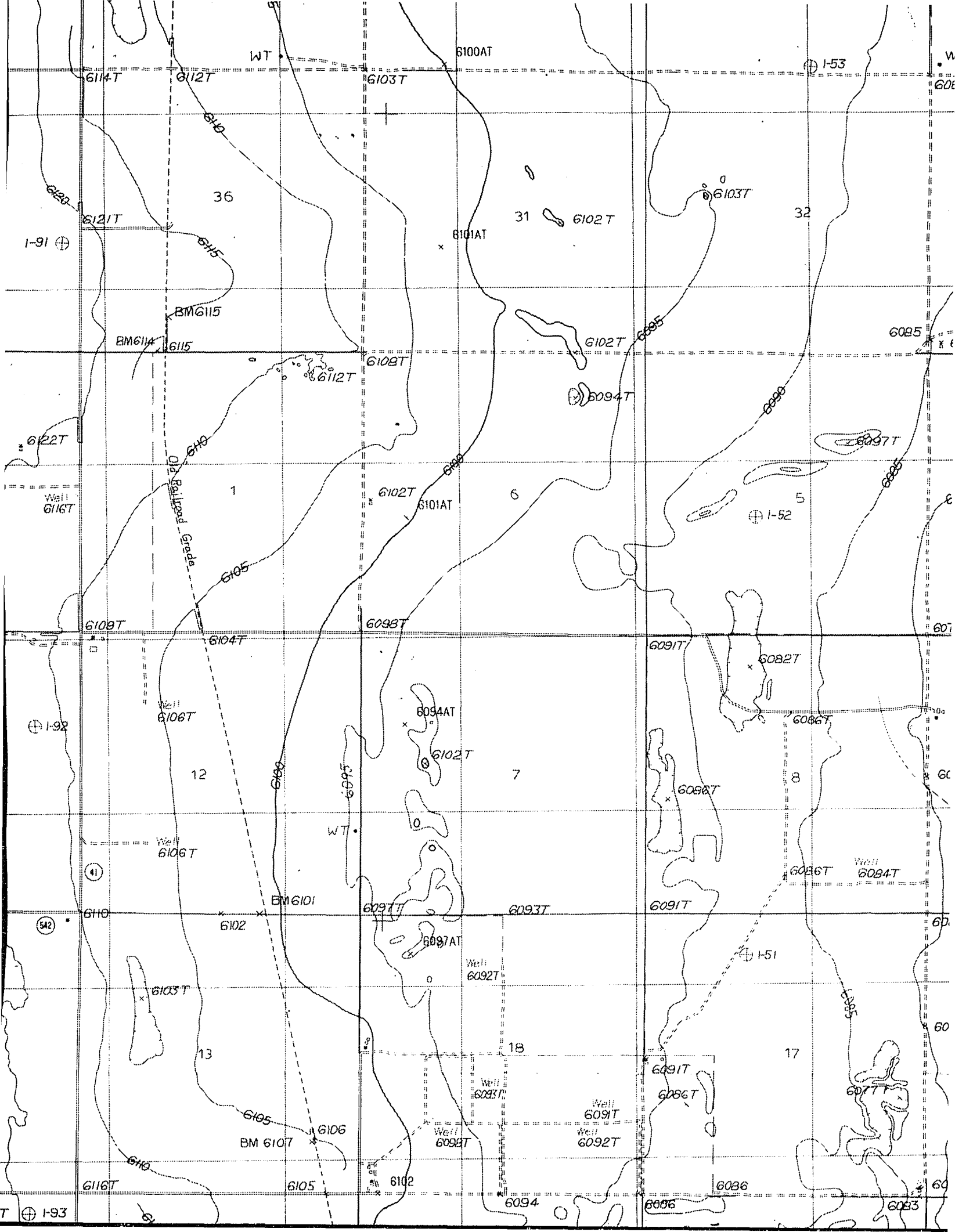






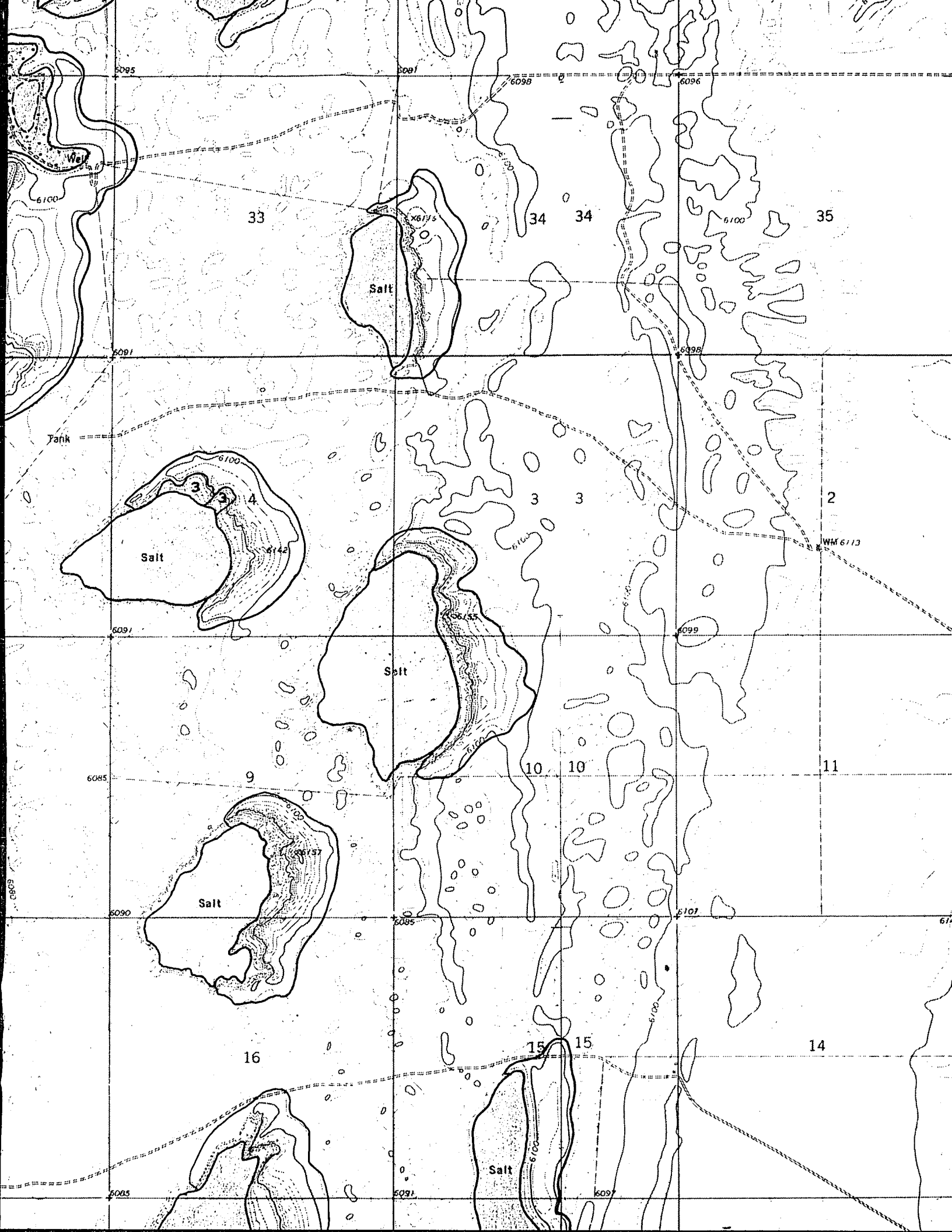






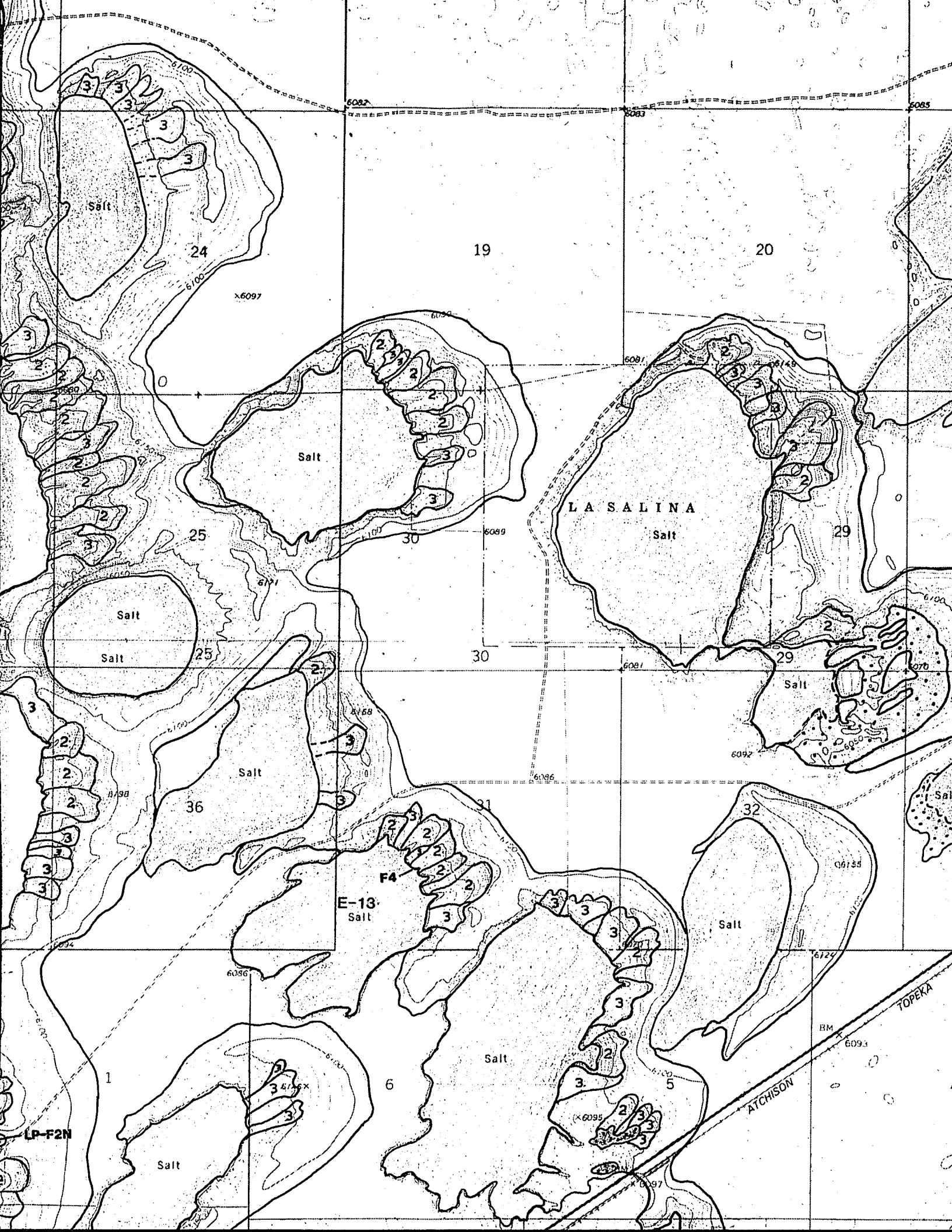


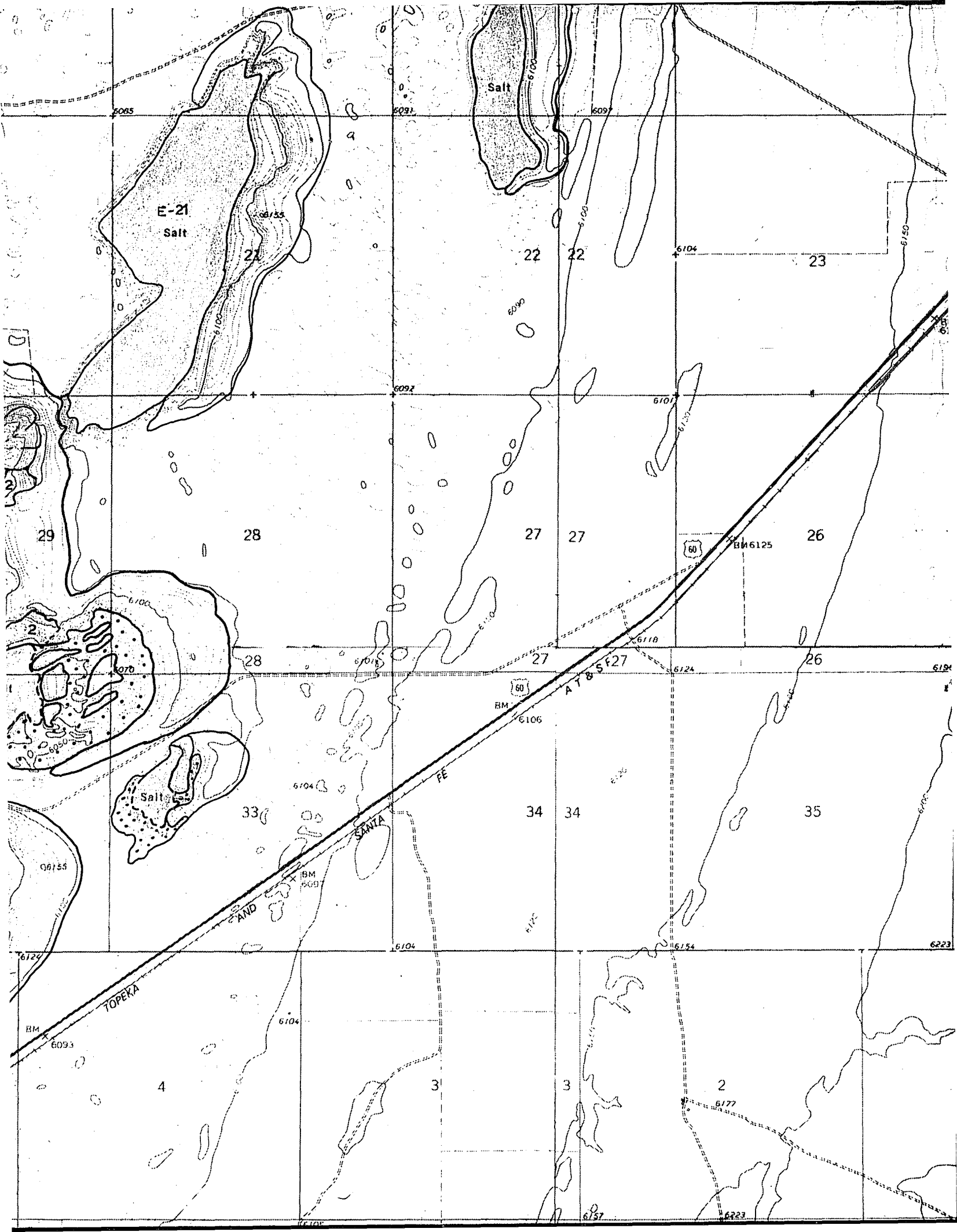








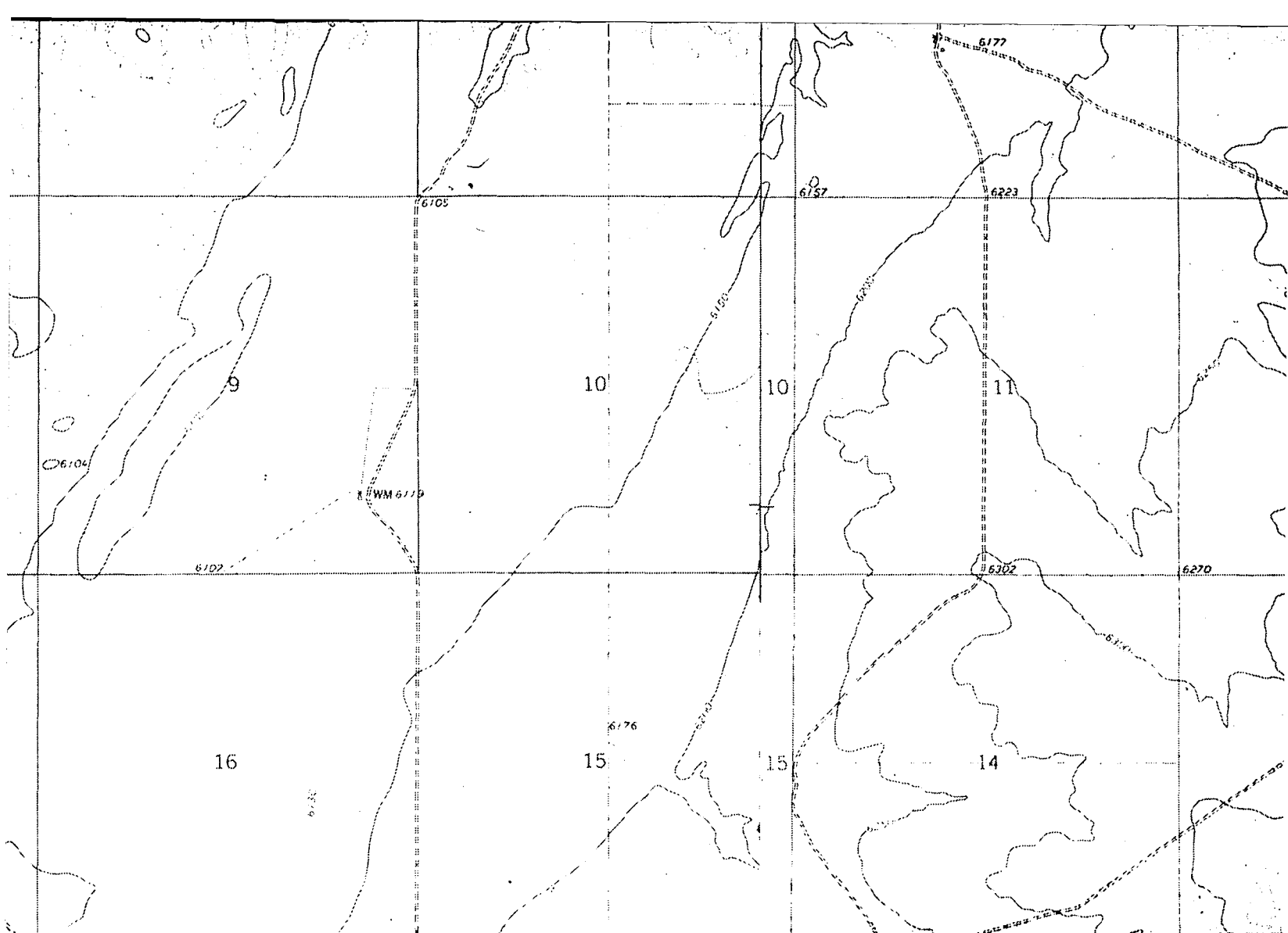












### EXPLANATION

Expanding on a 1:31,000 surficial geologic map of the Estancia Valley (Bachhuber, 1971), this map focuses on the deflation basins, dunes, and earthflow scars of the Willard Playa/Dune Complex.

#### Earthflows:

1

#### SLIGHTLY MODIFIED EARTHFLOW SCARS (TYPE 1)

Scars are easily discernible and original morphology is well preserved; scars exhibit long distinct sidewalls, sharp headwall crowns, and flat bottomed floors with a continuous slope. The scars are not extensively cut by arroyos or modified by eolian activity. These scars are the most recent.

2

#### MODIFIED EARTHFLOW SCARS (TYPE 2)

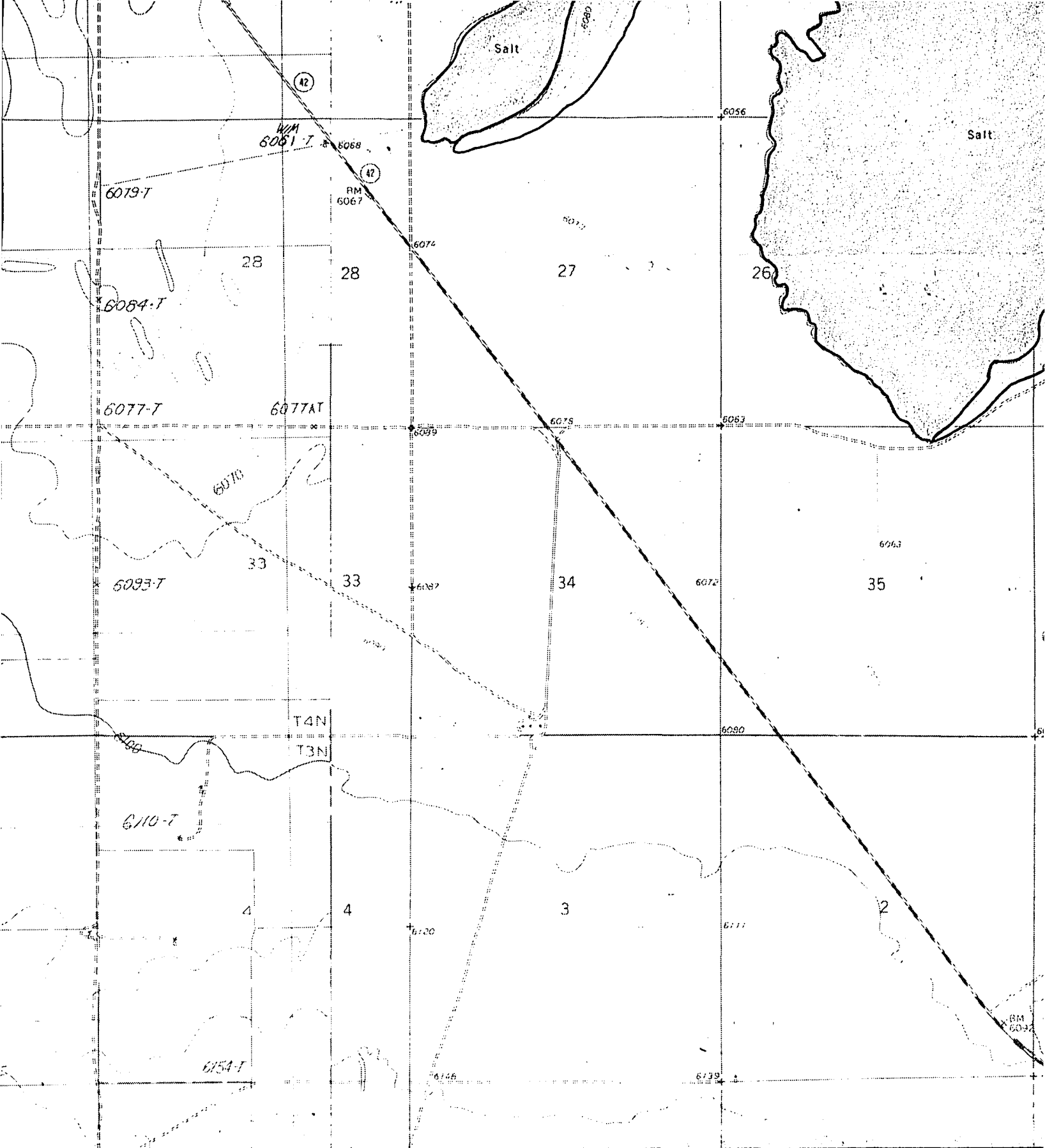
Discernible but original morphology modified by eolian activity and arroy cutting. Headwalls often appear as blowouts at the dune crest. Sidewalls are preserved but are modified and less distinct than type 1. Floors are more scalloped and dissected by arroyos.

3

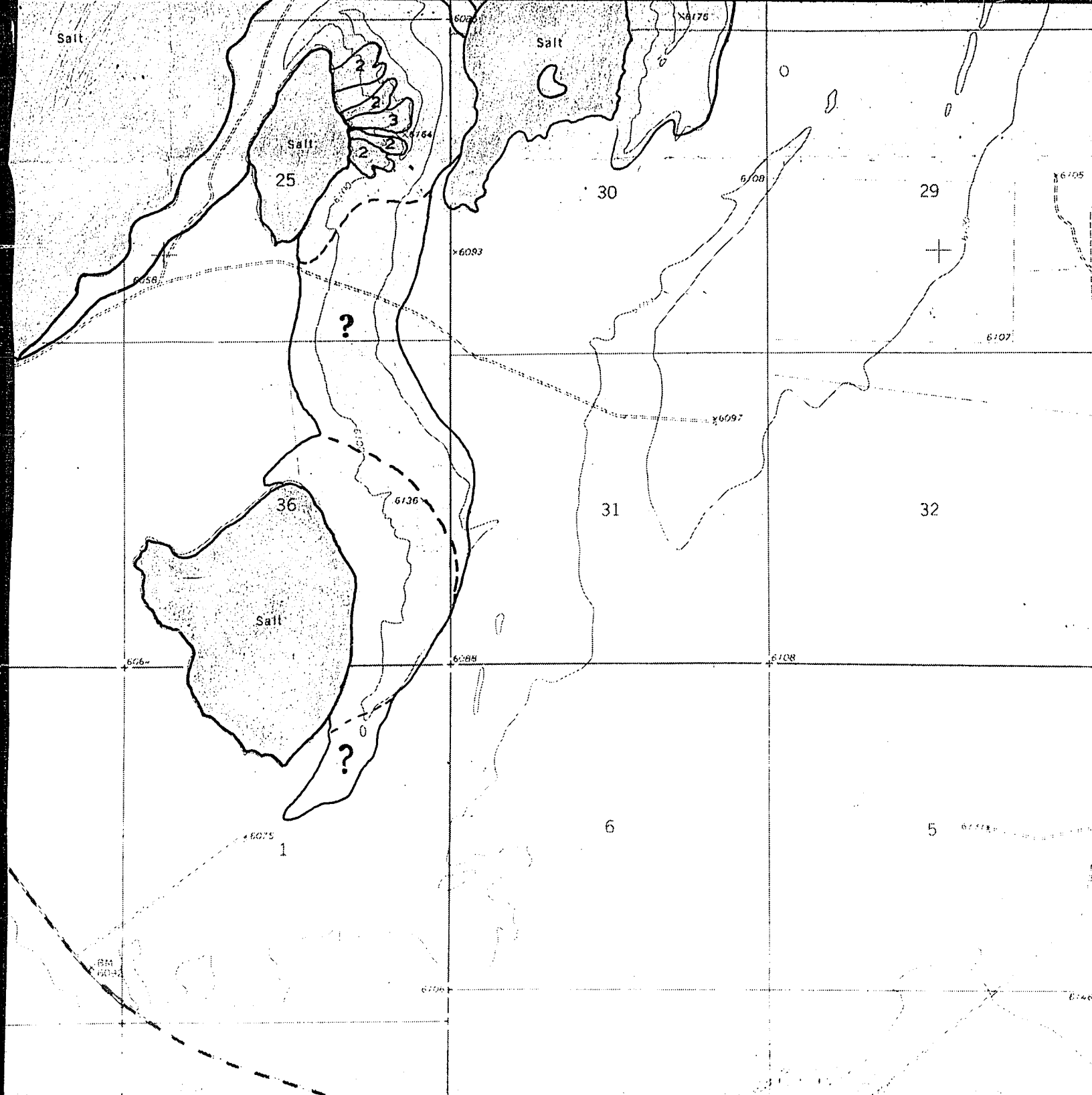
#### GREATLY MODIFIED EARTHFLOW SCARS (TYPE 3)

Not distinguishable from deflation scours. Original morphology highly obscured and modified by eolian activity. Head and sidewalls





# DWS OF THE WILLARD PLAYA/DUN



# DUNE COMPLEX, ESTANCIA VALLI

By

Kurt A. Goebel

1989

scars of the Willard Playa/Dune Complex.

Earthflows:



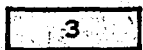
**SLIGHTLY MODIFIED EARTHFLOW SCARS (TYPE 1)**

Scars are easily discernible and original morphology is well preserved; scars exhibit long distinct sidewalls, sharp headwall crowns, and flat bottomed floors with a continuous slope. The scars are not extensively cut by arroyos or modified by eolian activity. These scars are the most recent.



**MODIFIED EARTHFLOW SCARS (TYPE 2)**

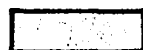
Discernible but original morphology modified by eolian activity and arroyo cutting. Headwalls often appear as blowouts at the dune crest. Sidewalls are preserved but are modified and less distinct than type 1. Floors are more scalloped and dissected by arroyos.



**GREATLY MODIFIED EARTHFLOW SCARS (TYPE 3)**

Not distinguishable from deflation scours. Original morphology highly obscured and modified by eolian activity. Head and sidewalls are not distinct and original dune slope is rarely preserved between adjacent flows. Floors are scalloped and dissected by arroyos.

Surficial and Geomorphic Units:



**WILLARD DUNES**

Coarse sand to fine silt-sized gypsum with 60% clay pellets; moderate sorting. Indistinctive small and large scale cross-bedding; gypsiferous units common. Sediments are derived from pre-existing Meinzer Dunes and underlying lacustrine sediments. Dune thickness attains 30 m; generally stabilized but with locally active areas.



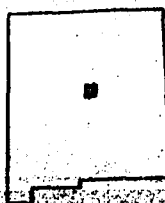
**PLAYA-FLOORED DEFLATION BASINS**

Silty-sand to clay, distinct laminae of organic, inorganic, and gypsiferous units. Generally, 0-1 m thick. Commonly encrusted with salt and/or gypsum. Forms floors of active deflation basins.

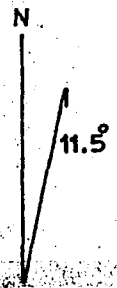


**DEFLATION BASIN FLOORS**

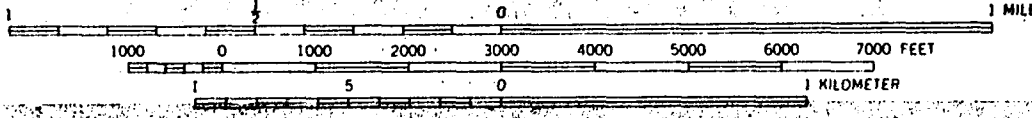
Partially vegetated and stable with minor topography. Forms floors of inactive deflation basins.



New Mexico



SCALE 1:24 000



**VALLEY, NEW MEXICO**